ELSEVIER

Coordination Chemistry Reviews 231 (2002) 23–46

COORDINATION CHEMISTRY REVIEWS

www.elsevier.com/locate/ccr

Advances in the chemistry of metallacarboranes of f-block elements

Zuowei Xie *

Department of Chemistry, The Chinese University of Hong Kong, Shatin NT, Hong Kong

Received 28 October 2001; received in revised form 10 February 2002

Contents

Abstract

The chemistry of metallacarboranes of f-block elements has experienced considerable growth in the past 10 years. The recent discovery of many novel complexes, interesting reactivity patterns and new bonding mode in this field has made this chemistry very attractive, diverse and unique. This review summarizes the development in this research field since the successful preparation of the first metallacarborane of f-block elements. Achievements, problems and perspectives are discussed in this article. © 2002 Elsevier Science B.V. All rights reserved.

Keywords: Actinacarborane; Actinide; Carborane; f-Element; Lanthanacarborane; Lanthanide; Metallacarborane; Rare earth

1. Introduction

The chemistry of metallacarboranes of d-block elements has witnessed an explosive growth since the first metallacarborane was reported in 1965 [1]. The progress in this field as well as metallacarboranes of s- and p-block elements has been extensively reviewed [2,3]. In sharp contrast, the chemistry of metallacarboranes of f-block elements is less explored and no comprehensive reviews and monographs on this subject have appeared in the literature [2,3].

With today's more sophisticated experimental and analytical techniques and encouraged by the exciting chemistry of organo-f-element compounds [4], considerable progress has been made since the 1990s in the chemistry of metallacarboranes of f-block elements. This review summarizes the development of this growing field. Metallacarboranes of scandium and yttrium are included in this review for comparisons since their chemical and physical properties are often similar to those of lanthanides.

* Tel.: +852-260-96269; fax: +852-260-35057
E-mail address: zxie@cuhk.edu.hk (Z. Xie).

0010-8545/02/$ - see front matter
PII: S0010-8545(02)00112-1

2. Metallacarboranes of lanthanides

2.1. C_2B_9 systems

Recognition of the isolobal analogue between the cyclopentadienyl ($C_5H_5^-$) and dicarbollide ion ($C_2B_9H_{11}^{2-}$) initiated the field of metallacarborane chemistry [5], and subsequently led to the synthesis of the first metallacarboranes of lanthanides (η^5-$C_2B_9H_{11}$)Ln(THF)$_4$ (Ln = Sm, Yb) (often called lanthanacarboranes) (Scheme 1) [6]. The coordinated THF molecules in these complexes are labile and can be replaced by other strong coordinating solvents such as DMF and CH_3CN. The solid-state structure of (η^5-$C_2B_9H_{11}$)Yb(DMF)$_4$ has been subjected to X-ray analyses, shown in Fig. 1. It is a half-sandwich complex in which the Yb^{2+} ion is η^5-bonded to the five-membered ring of $C_2B_9H_{11}^{2-}$ ligand with an average Yb-cage atom distance of 2.74 Å.

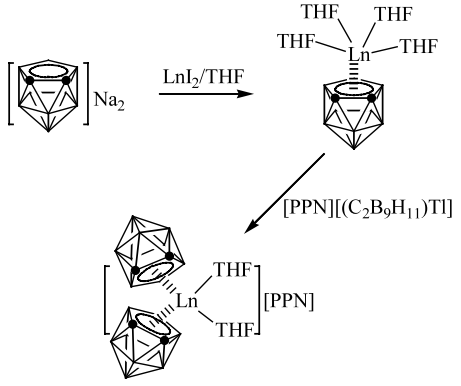

Ln = Sm, Yb

Scheme 1.

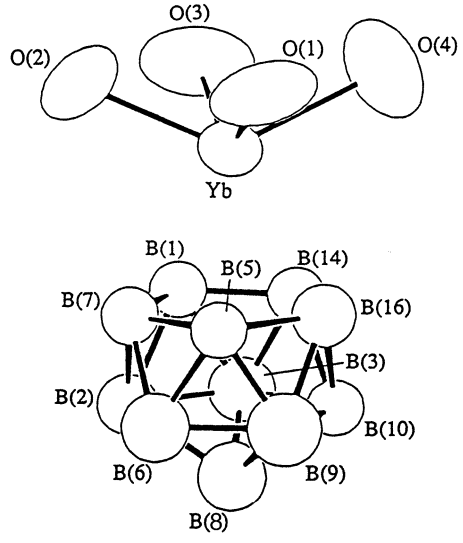

Fig. 1. Structure of (η^5-$C_2B_9H_{11}$)Yb(DMF)$_4$ [6].

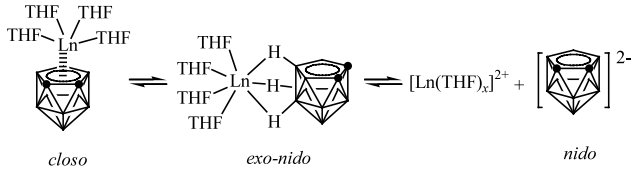

Scheme 2.

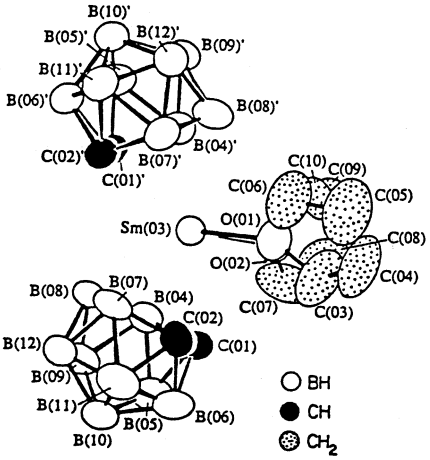

Fig. 2. Structure of [(η^5-$C_2B_9H_{11}$)$_2$Sm(THF)$_2$]$^-$ [7].

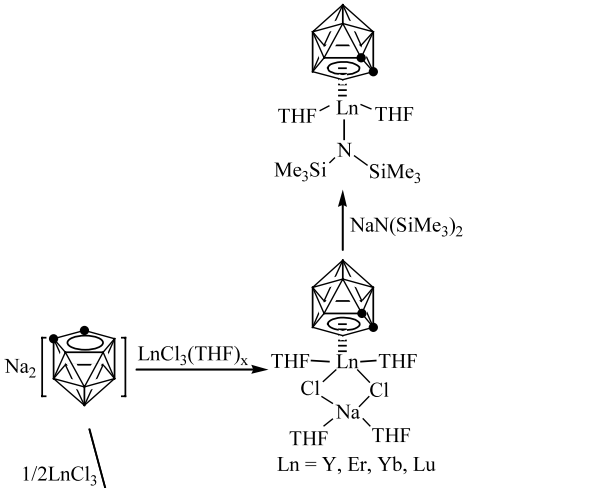

Ln = La, Sm, Y, Er, Yb, Lu

Scheme 3.

These complexes are fluxional in THF solution and the following equilibrium has been established on the basis of variable-temperature ^{11}B-NMR study (Scheme 2) [7].

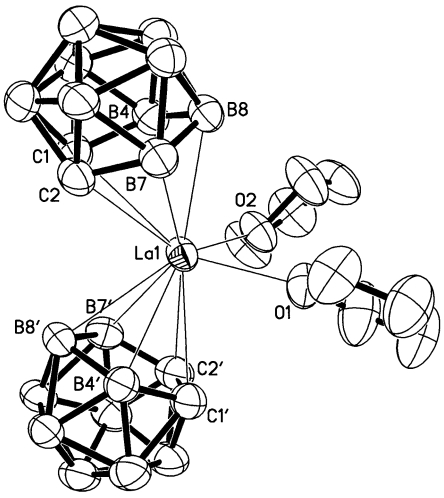

Fig. 3. Structure of $[(\eta^5\text{-}C_2B_9H_{11})_2La(THF)_2]^-$ [9].

Like other Ln(II) complexes [4,8], $(\eta^5\text{-}C_2B_9H_{11})Ln(THF)_4$ can be oxidized by $[PPN][(C_2B_9H_{11})Tl]$ (PPN = $[(C_6H_5)_3P]_2N$) in THF to form the full-sandwich lanthanacarboranes $[PPN][(\eta^5\text{-}C_2B_9H_{11})_2Ln(THF)_2]$ (Ln = Sm, Yb) (Scheme 1) [6,7]. As shown in Fig. 2, the Sm^{3+} ion is η^5-bonded to two $C_2B_9H_{11}^{2-}$ ligands and σ-bonded to two THF molecules in a distorted-tetrahedral geometry with an average Sm–cage atom distance of 2.735 Å and a ring centroid–Sm–ring centroid angle of 131.9°.

The full-sandwich lanthanacarboranes can also be prepared by direct salt metathesis between $LnCl_3$ and $Na_2[C_2B_9H_{11}]$ in THF in a molar ratio of 1:2 (Scheme 3) [9,10]. Such a methodology makes the preparation of metallacarboranes of all lanthanides possible [10]. An X-ray analysis reveals that the La complex is isostructural with its Sm analogue, shown in Fig. 3. The average La–cage atom distance is 2.804(5) Å and the ring centroid–La–ring centroid angle is 132.7°. These measured values are comparable to those found in organolanthanum complexes of the type $(C_5Me_5)_2LaL$ [11].

These full-sandwich lanthanacarboranes do not have the functional groups, which limits further exploration of their chemical properties. For this reason, the preparation of lanthanacarboranes containing Ln–Cl bond is of interest. In this connection, an equimolar reaction between the THF-solvated complexes $LnCl_3(THF)_x$ and $Na_2[C_2B_9H_{11}]$ in THF is found to give half-sandwich lanthanacarborane chloride complexes of the general formula $(\eta^5\text{-}C_2B_9H_{11})Ln(THF)_2(\mu\text{-}Cl)_2Na(THF)_2$ (Ln = Y, Er, Yb, Lu) in a typical yield of 45% (Scheme 3) [12]. It is noted that only full-sandwich lanthanacarboranes are isolated for early lanthanides regardless of the molar ratio of reactants due to the ligand redistribution reactions. This type of half-sandwich lanthanacarborane chlorides furnishes important intermediates for the preparation of complexes containing Ln–C, Ln–N, and Ln–O bonds. As

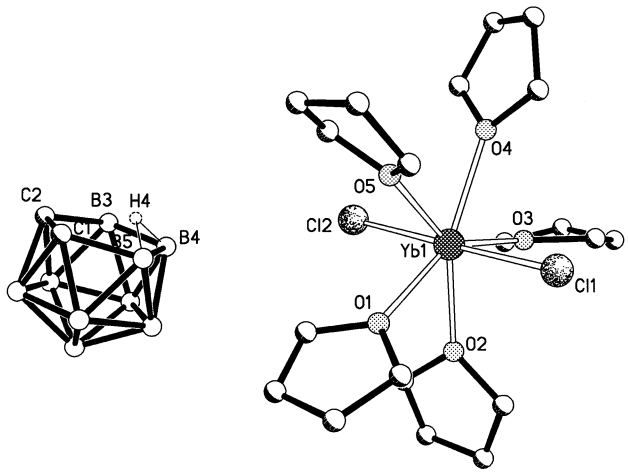

Fig. 4. Structure of $[YbCl_2(THF)_5][nido\text{-}C_2B_9H_{12}]$ [12].

shown in Scheme 3, treatment of $(\eta^5\text{-}C_2B_9H_{11})Ln(THF)_2(\mu\text{-}Cl)_2Na(THF)_2$ with 1 equiv. of $Na_2[C_2B_9H_{11}]$ or $NaN(SiMe_3)_2$ affords the corresponding full-sandwich lanthanacarboranes $\{(\eta^5\text{-}C_2B_9H_{11})_2Ln(THF)_2\}\{Na(THF)_2\}$ or half-sandwich lanthanacarboranes $(\eta^5\text{-}C_2B_9H_{11})LnN(SiMe_3)_2(THF)_2$, respectively [10,12]. Partial hydrolysis of $(\eta^5\text{-}C_2B_9H_{11})Ln(THF)_2(\mu\text{-}Cl)_2Na(THF)_2$ yields ionic complexes $[LnCl_2(THF)_5][nido\text{-}C_2B_9H_{12}]$ (Ln = Y, Yb). Their solid-state structures have been confirmed by single-crystal X-ray analyses, shown in Fig. 4. These results support the proposed structures of their parent complexes. The presence of the doubly bridging Cl unit $Ln(\mu\text{-}Cl)_2Na$ can enhance the stability of the half-sandwich lanthanacarborane chlorides.

Reaction of $[(\eta^5\text{-}C_5Me_5)ScCl_2]_x$ with 1 equiv. of $Na_2[C_2B_9H_{11}]$ or treatment of $[(\eta^5\text{-}C_5Me_5)ScMe_2]_x$ with 1 equiv. of $C_2B_9H_{13}$ affords the same mixed

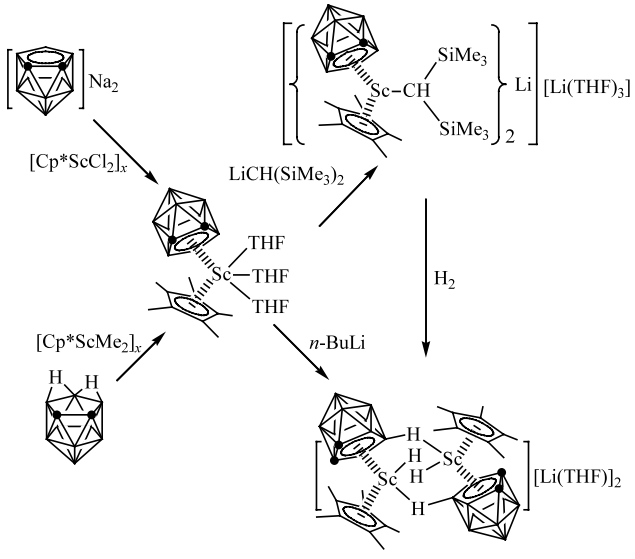

Scheme 4.

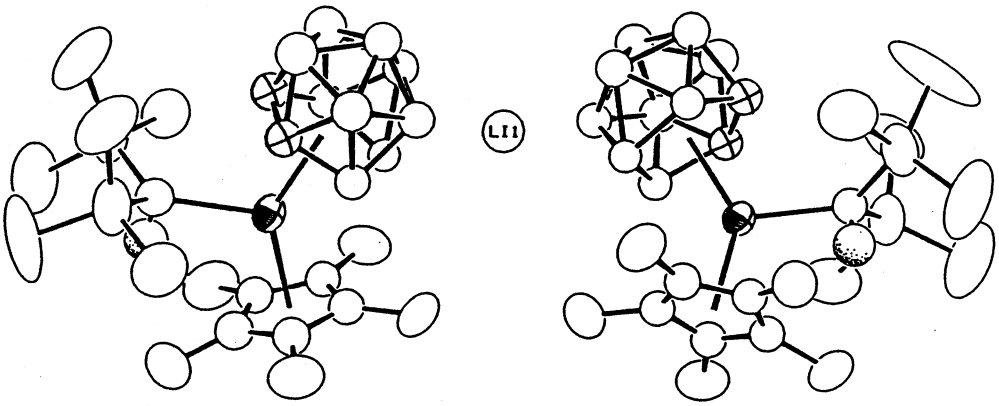

Fig. 5. Structure of $\{[\{(\eta^5\text{-}C_5Me_5)(\eta^5\text{-}C_2B_9H_{11})\}ScCH(SiMe_3)_2]_2Li\}^-$ [13].

sandwich complex $[(\eta^5\text{-}C_5Me_5)(\eta^5\text{-}C_2B_9H_{11})]Sc(THF)_3$. This neutral scandacarborane can further react with an equimolar amount of $LiCH(SiMe_3)_2$ to give the corresponding alkyl derivative $\{[\{(\eta^5\text{-}C_5Me_5)(\eta^5\text{-}C_2B_9H_{11})\}ScCH(SiMe_3)_2]_2Li\}\{Li(THF)_3\}$. Reaction of this alkyl complex with H_2 generates the metal hydride $\{[(\eta^5\text{-}C_5Me_5)(\eta^5\text{-}C_2B_9H_{11})]ScH\}_2\{Li(THF)\}_2$. This hydride can also be prepared by the reaction of $[(\eta^5\text{-}C_5Me_5)(\eta^5\text{-}C_2B_9H_{11})]Sc(THF)_3$ with 1 equiv. of *n*-BuLi. These transformations are summarized in Scheme 4 [13].

Figs. 5 and 6 show the solid-state structures of the alkyl and hydride derivatives, respectively. Both consist of a bent-metallocene structural motif in which the Sc^{3+} ion is η^5-bonded to one $C_2B_9H_{11}^{2-}$ and one $C_5Me_5^-$, respectively. In addition, the Sc^{3+} ion is σ-bonded to $CH(SiMe_3)_2$ in the alkyl derivative and to two H atoms from terminal hydrido group and the BH unit of the neighboring carborane cage, respectively, in the hydride derivative. The average Sc–cage atom distance of 2.514(15) Å is very close to the average Sc–C(C_5Me_5)

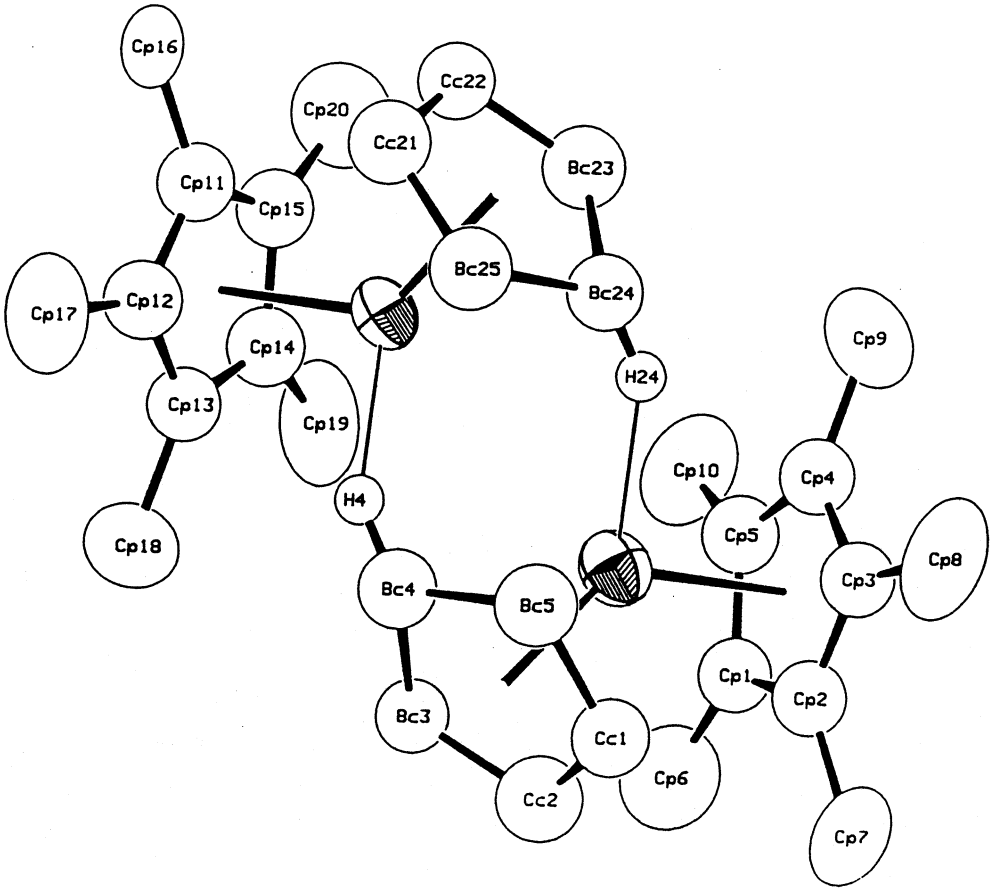

Fig. 6. Structure of $\{[(\eta^5\text{-}C_5Me_5)(\eta^5\text{-}C_2B_9H_{11})]ScH\}_2^{2-}$ [13].

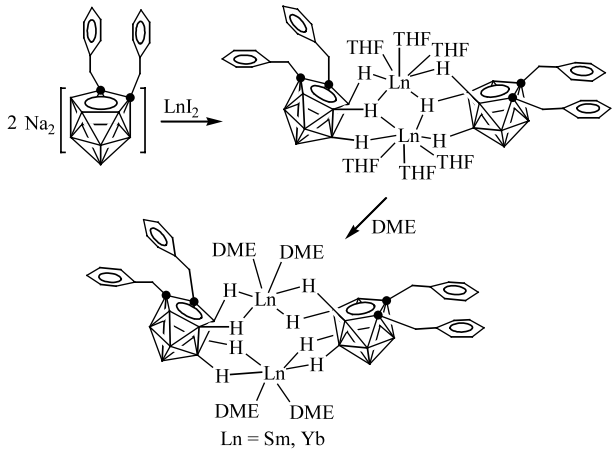

Scheme 5.

distance of 2.499(13) Å, suggesting similar ligating ability of the two π-bonding ligands. It is noteworthy that the tremendous stability of the dimeric scandium hydride $\{[(\eta^5\text{-}C_5Me_5)(\eta^5\text{-}C_2B_9H_{11})]ScH\}_2\{Li(THF)\}_2$ makes it inert toward PMe_3, 2-butyne, ethylene and propene.

Substituents on the bonding face of $C_2B_9H_{11}^{2-}$ ligand have very large effects on the bonding interactions between lanthanide ions and the ligand, in contrast to its isolobal analogue $C_5H_5^-$. Reaction of LnI_2 with 1 or 2 equiv. of $Na_2[nido\text{-}(C_6H_5CH_2)_2C_2B_9H_9]$ in THF gives $[exo\text{-}nido\text{-}\{(C_6H_5CH_2)_2C_2B_9H_9\}Ln(THF)_3]_2$ (Ln = Sm, Yb) in good yield. No 1:2 (Ln to ligand) complexes are isolated though excess ligands are present in the reaction system (Scheme 5) [14]. Recrystallization from a DME/THF solution affords the corresponding DME coordinated complexes [9]. These *exo-nido*-lanthanacarboranes have been fully characterized by various spectroscopic data and X-ray diffraction studies. The

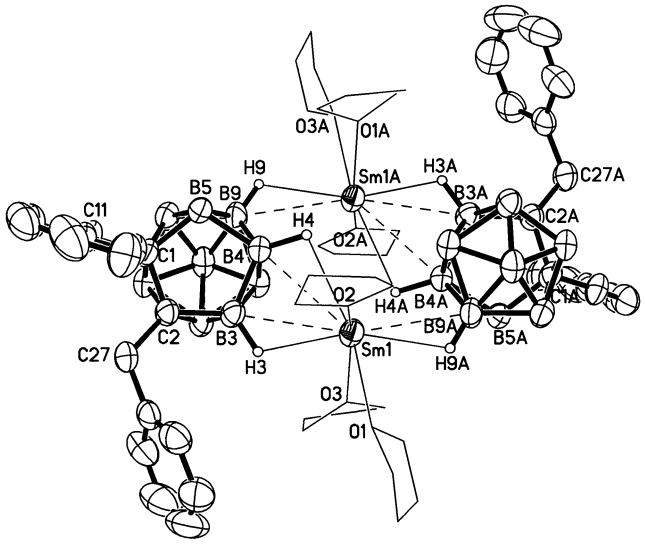

Fig. 7. Structure of $[exo\text{-}nido\text{-}\{(C_6H_5CH_2)_2C_2B_9H_9\}Sm(THF)_3]_2$ [14].

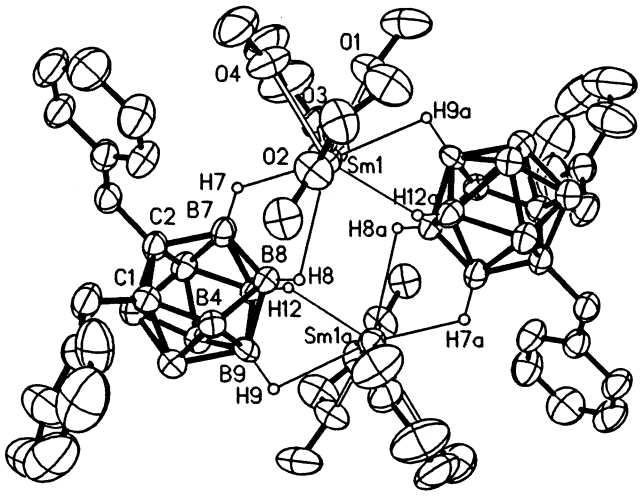

Fig. 8. Structure of $[exo\text{-}nido\text{-}\{(C_6H_5CH_2)_2C_2B_9H_9\}Sm(DME)_2]_2$ [9].

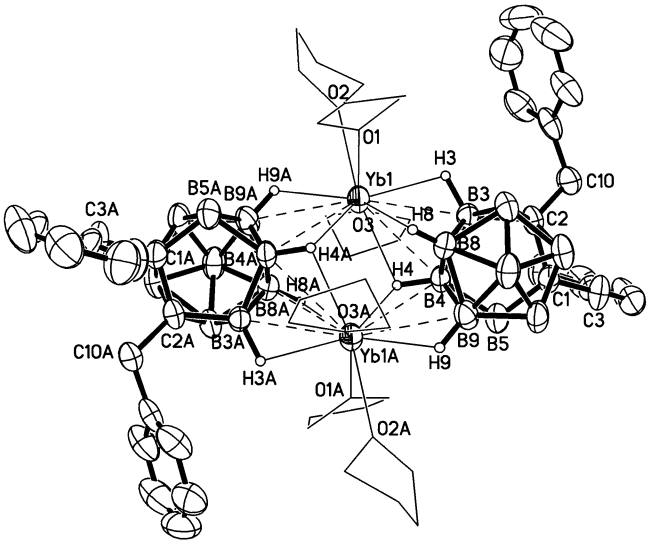

Fig. 9. Structure of $[exo\text{-}nido\text{-}\{(C_6H_5CH_2)_2C_2B_9H_9\}Yb(THF)_3]_2$ [14].

main structural features are the presence of exclusive Ln–H–B bondings between Ln ions and carboranyl ligands and the coordination sphere around Ln being completed by either THF or DME molecules. The coordination details between Ln and $[nido\text{-}(C_6H_5CH_2)_2C_2B_9H_9]^{2-}$ are slightly different from each other (Figs. 7–9). The average Sm···B distances are 3.066(5) and 3.042(8) Å in THF and DME coordinated complexes, respectively. The average Yb···B distance is 2.929(8) Å in the Yb analogue. The isolation of these *exo-nido*-lanthanacarboranes strongly supports the fluxional phenomenon observed in the THF solution of $(\eta^5\text{-}C_2B_9H_{11})Ln(THF)_4$ [7].

These results indicate that steric factors play a key role in the formation of *exo-nido*-lanthanacarboranes, or dominate the coordination mode between metal ions and carboranyl ligands, showing the differences between

$C_2B_9H_{11}^{2-}$ and $C_5H_5^-$ ligands in bonding with transition metal ions.

Interaction between $La(ClO_4)_3$ and 2 equiv. of $Li_2[(MeOCH_2)_2C_2B_9H_9]$ in THF giving, after treatment with $[C_6H_5CH_2NMe_3]Cl$, $[\{(MeOCH_2)_2C_2B_9H_9\}_2La(THF)_2][C_6H_5CH_2NMe_3]$ is reported with no structural data [15]. The preliminary report on the preparation of $[(\eta^5\text{-}C_2B_9H_{11})_2Gd][Na(THF)]$ fails to confirm its molecular structure [16].

2.2. C_2B_{10} systems

2.2.1. *nido*-C_2B_{10} systems

It has been well-documented that *o*-$R_2C_2B_{10}H_{10}$ (R = H, alkyl, aryl) can be readily reduced by alkali metals to form M_2[*nido*-$R_2C_2B_{10}H_{10}$] which are very useful versatile synthons for the production of numerous metallacarboranes of s-, p-, and d-elements [2,3]. Treatment of $LnI_2(THF)_2$ with 1 equiv. of Na_2[*nido*-$C_2B_{10}H_{12}$] in THF results in the isolation of half-sandwich lanthanacarboranes $[(\eta^6\text{-}C_2B_{10}H_{12})Ln(THF)_x]_n$ ($x = 3$, $n = \infty$, Ln = Sm, Eu; $x = 4$, $n = 1$, Ln = Yb) (Scheme 6) [17]. Recrystallization of the Eu complex from MeCN/Et_2O gives a MeCN coordinated species $[(\eta^6\text{-}C_2B_{10}H_{12})Eu(MeCN)_3]_n$. Its polymeric nature has been confirmed by single-crystal X-ray analyses. Each Eu^{2+} ion is η^6-bonded to one $C_2B_{10}H_{12}^{2-}$ ligand and σ-bonded to three MeCN molecules and two H–E (E = cage B and C atoms) bonds from the neighboring carboranyl ligand in a highly distorted-octahedral geometry, shown in Fig. 10. The average Eu–N and Eu–cage atom distances are 2.677(9) and 2.983(11) Å, respectively.

The half-sandwich complex $[(\eta^6\text{-}C_2B_{10}H_{12})Eu(THF)_3]_n$ does not react with neutral nucleophiles such as CO, phosphines, alkenes, and alkynes. It, however, can react with another molar amount of Na_2[*nido*-$C_2B_{10}H_{12}$] in THF to form, after treatment with Et_4NCl, a full-sandwich lanthanacarborane $[Et_4N]_2[(\eta^6\text{-}C_2B_{10}H_{12})_2Eu(THF)_2]$ [17,18]. This complex can also

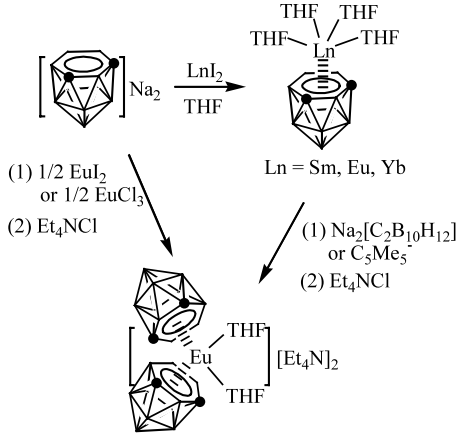

Scheme 6.

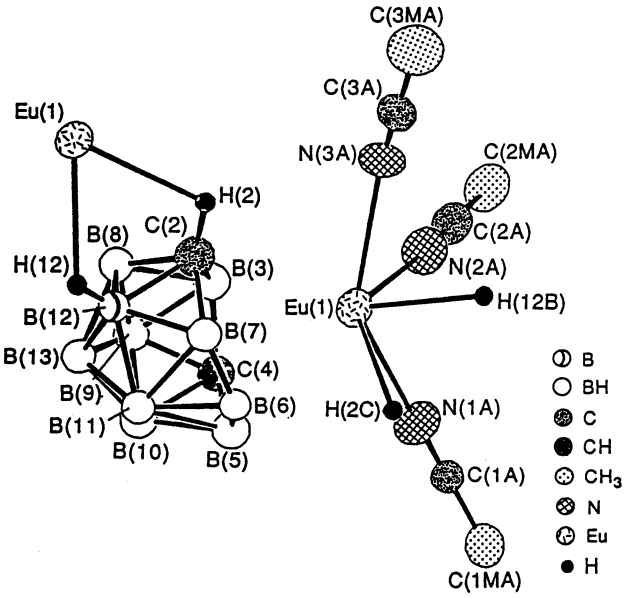

Fig. 10. Structure of $[(\eta^6\text{-}C_2B_{10}H_{12})Eu(MeCN)_3]_n$ [18].

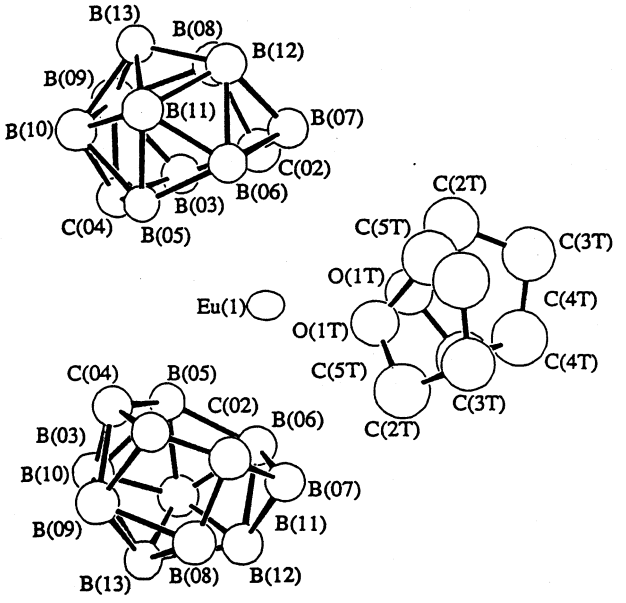

Fig. 11. Structure of $[(\eta^6\text{-}C_2B_{10}H_{12})_2Eu(THF)_2]^{2-}$ [18].

be prepared by either the reaction of $EuCl_3$ with 2 equiv. of *nido*-$C_2B_{10}H_{12}^{2-}$ or treatment of $[(\eta^6\text{-}C_2B_{10}H_{12})Eu(THF)_3]_n$ with an equimolar amount of $C_5Me_5^-$ in THF (Scheme 6). These results indicate that (1) *nido*-$C_2B_{10}H_{12}^{2-}$ is a strong reducing agent which can reduce Eu^{3+} to Eu^{2+} and (2) $[(\eta^6\text{-}C_2B_{10}H_{12})(\eta^5\text{-}C_5Me_5)Eu(THF)_2]^-$ is unstable leading to the formation of $[(\eta^6\text{-}C_2B_{10}H_{12})_2Eu(THF)_2]^{2-}$ and $(\eta^5\text{-}C_5Me_5)_2Eu(THF)_2$. As shown in Fig. 11, the Eu^{2+} ion is η^6-bonded to two $C_2B_{10}H_{12}^{2-}$ ligands and σ-bonded to two THF molecules in a distorted-tetrahedral geometry with a ring centroid–Eu–ring centroid angle of

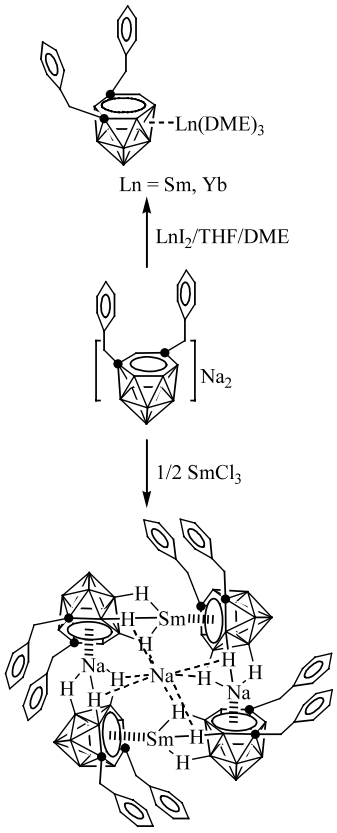

Scheme 7.

127.4(3)°. The average Eu–cage atom and Eu–O distances are 3.03(1) and 2.63(1) Å, respectively.

Treatment of LnI_2 with 1 equiv. of $[(C_6H_5CH_2)_2C_2B_{10}H_{10}]K_2(THF)_4$ [19] in THF at room temperature gives, after recrystallization from DME, *exo-nido*-lanthanacarboranes *exo-nido*-$[(C_6H_5CH_2)_2C_2B_{10}H_{10}]Ln(DME)_3$ (Ln = Sm, Yb) (Scheme 7), implying that steric effects dominate the coordination mode between the central metal ions and carboranyl ligands [14]. Their solid-state structures are shown in Figs. 12 and 13, respectively. They are isomorphous but not isostructural. The common structural features are (1) the monomeric *exo-nido* structures formed by exclusive Ln–H–B bondings between the Ln^{2+} ion and carborane ligand and (2) the coordination sphere around Ln metal being completed by three DME molecules. The coordination details between Ln and $[nido\text{-}(C_6H_5CH_2)_2C_2B_{10}H_{10}]^{2-}$ are, however, slightly different in the two compounds. Thus the $[nido\text{-}(C_6H_5CH_2)_2C_2B_{10}H_{10}]^{2-}$ anion is bonded to Sm^{2+} via three B–H bonds, one from the open hexagonal C_2B_4 face and the other two from the pentagonal belt (B_5); whereas this anion bonds to Yb^{2+} through two B–H bonds from the open hexagonal C_2B_4 face only. This difference is an apparent consequence of the different sizes of the Ln ions. The average Sm···B and Yb···B distances are 3.037(3) and 2.894(7) Å, respectively. Reaction of LnI_2 with 2 equiv. of $[(C_6H_5CH_2)_2C_2B_{10}H_{10}]Na_2(THF)_4$ affords lanthanacarboranes which have been formulated as $[(C_6H_5CH_2)_2C_2B_{10}H_{10}]_4Ln_2Na_4(THF)_2$ (Ln = Sm, Yb) on the basis of spectroscopic data and elemental analyses. The bonding interactions between the central metal ions and carboranyl ligands in these complexes are not very clear.

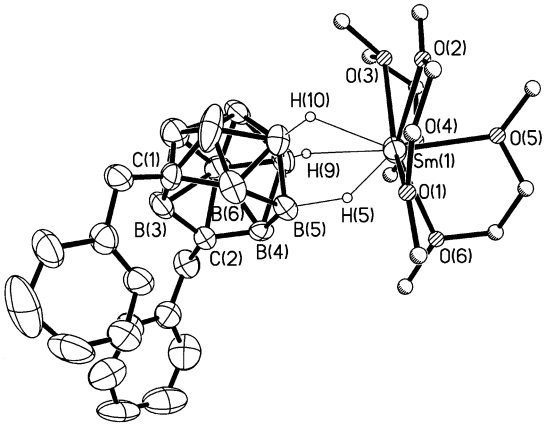

Fig. 12. Structure of *exo-nido*-$[(C_6H_5CH_2)_2C_2B_{10}H_{10}]Sm(DME)_3$ [14].

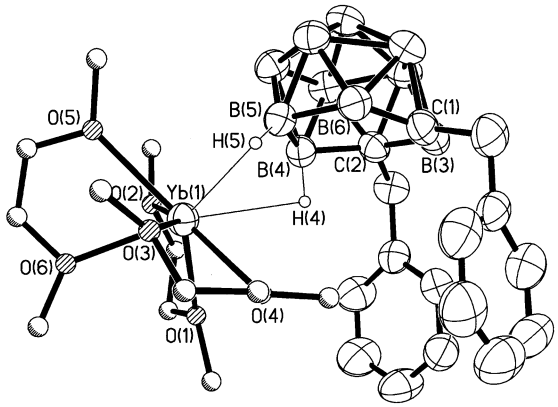

Fig. 13. Structure of *exo-nido*-$[(C_6H_5CH_2)_2C_2B_{10}H_{10}]Yb(DME)_3$ [14].

Reaction of $YbCl_3$ with 2 equiv. of $[(C_6H_5CH_2)_2C_2B_{10}H_{10}]Na_2(THF)_4$ [14] in THF/DME leads to the isolation of *exo-nido*-$[(C_6H_5CH_2)_2C_2B_{10}H_{10}]Yb(DME)_3$. However, treatment of $SmCl_3$ with 2 equiv. of $[(C_6H_5CH_2)_2C_2B_{10}H_{10}]Na_2(THF)_4$ in THF affords an unprecedented cluster *closo-exo*-$[(C_6H_5CH_2)_2C_2B_{10}H_{10}]_4Sm_2Na_3$ (Scheme 7) [14]. It is a mixed-valence samaracarborane containing both Sm^{3+} and Sm^{2+} centers. An X-ray diffraction study reveals that this novel cluster consists of a central sodium atom that bonds to four half-sandwich $[\eta^6\text{-}(C_6H_5CH_2)_2C_2B_{10}H_{10}]M$ (M = Na, Sm) units in a distorted-tetrahedral arrangement via four sets of two B–H bonds from the open hexagonal C_2B_4 bonding face at an average Na···B distance of 3.050(5) Å (Fig. 14). The four 13-vertex half-sandwich $[\eta^6\text{-}(C_6H_5CH_2)_2C_2B_{10}H_{10}]M$ units are then connected to each other by four sets of three B–

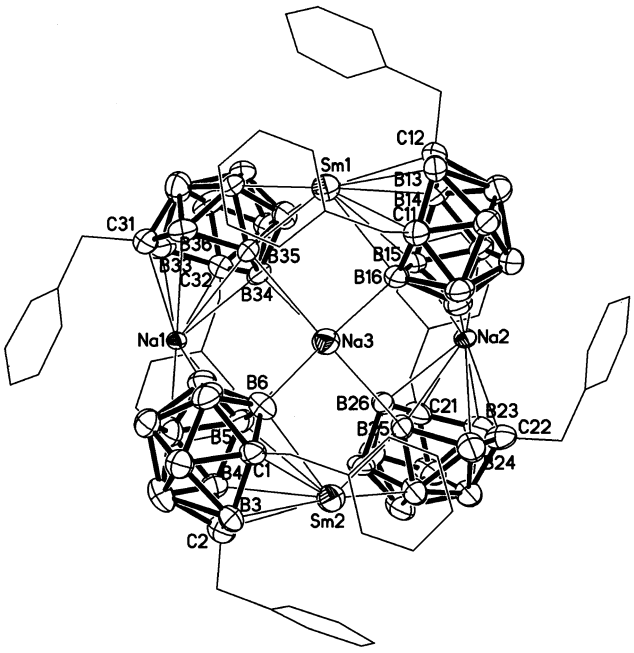

Fig. 14. Structure of *closo-exo*-$[(C_6H_5CH_2)_2C_2B_{10}H_{10}]_4Sm_2Na_3$ [14].

H–M bonds, one B–H bond from the open hexagonal C_2B_4 bonding face and the other two from the pentagonal belt. The average Sm(1)–cage(1) atom and Sm(1)···B (B_3 face) distances of 2.970(5) and 3.013(5) Å are very close to the corresponding Sm(2)–cage(2) atom and Sm(2)···B (B_3 face) distances of 2.968(5) and 3.037(5) Å, respectively. The average Na(1)–cage(3) atom and Na(1)···B (B_3 face) distances of 2.925(6) and 3.023(6) Å are also very close to the corresponding Na(2)–cage(4) atom and Na(2)···B (B_3 face) distances of 2.906(6) and 2.963(6) Å, respectively. On the other hand, the Sm^{3+} and Na^+ ions appear to have some interactions with the aromatic rings of the benzyl substituents. These results indicate that the coordination environment for all four Na(1), Na(2), Sm(1) and Sm(2) atoms is almost identical and two Sm ions are indistinguishable in terms of bond distances. The formal oxidation state for each Sm ion should then be +2.5. The formation of this mixed-valence samarium compound may be due to the incomplete reduction of Sm(III) by [*nido*-$(C_6H_5CH_2)_2C_2B_{10}H_{10}]^{2-}$ anion.

It has been previously discussed that $[(\eta^6\text{-}C_2B_{10}H_{12})(\eta^5\text{-}C_5Me_5)Eu(THF)_2]^-$ is unstable and undergoes ligand redistribution to form homoleptic Eu complexes [18]. To prevent such a ligand redistribution reaction, a Me_2Si-bridged ligand bearing both carboranyl and Cp groups has been designed and prepared [20]. Treatment of $NdCl_3$ with an equimolar amount of $[Me_2Si(C_5H_4)(C_2B_{10}H_{11})]K_3$ in THF at room temperature gives a yellowish-green air- and moisture-sensitive mixed sandwich lanthanacarborane $[\eta^5\text{:}\eta^6\text{-}Me_2Si(C_5H_4)(C_2B_{10}H_{11})]Nd(THF)_2$. It can also be prepared from the reaction of $[\eta^5\text{-}Me_2Si(C_5H_4)(C_2B_{10}H_{11})]NdCl_2(THF)_3$ with 2 equiv. of K metal in THF, which involves the redox reaction between K metal and carborane followed by an intramolecular salt metathesis reaction [20,21] (Scheme 8). Under similar reaction conditions, reaction of $LnCl_3$ (Ln = Sm, Yb) with $[Me_2Si(C_5H_4)(C_2B_{10}H_{11})]K_3$ in a molar ratio of 1:1 in THF, however, does not afford the analogous compounds of Nd; instead organolanthanide(II) complexes $\{[\eta^5\text{:}\eta^6\text{-}Me_2Si(C_5H_4)(C_2B_{10}H_{11})]Ln(THF)_2\}\text{-}\{K(THF)_2\}$ (Ln = Sm, Yb) are isolated. These results indicate that $[Me_2Si(C_5H_4)(C_2B_{10}H_{11})]^{3-}$ can reduce both Sm^{3+} and Yb^{3+} to Sm^{2+} and Yb^{2+}, respectively.

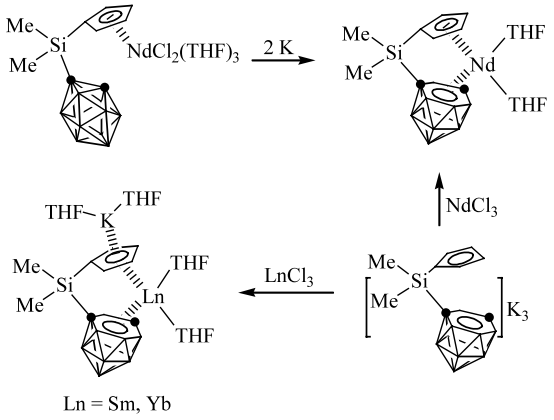

Scheme 8.

It seems rather difficult to prepare the trivalent Sm and Yb analogues incorporating the $C_2B_{10}H_{12}^{2-}$ ligand by the salt metathesis reactions owing to the reducing property of $C_2B_{10}H_{12}^{2-}$ and the oxidizing ability of the Sm(III) and Yb(III) ions. A new methodology is definitely desirable. Interestingly, treatment of a THF solution of SmI_2 with 2 equiv. of $[Me_2Si(C_5H_4)\text{-}(C_2B_{10}H_{11})]Na$ at room temperature gives an unprecedented trivalent samaracarborane $[\eta^5\text{:}\eta^6\text{-}Me_2\text{-}Si(C_5H_4)(C_2B_{10}H_{11})]Sm(THF)_2$ [21,22] (Scheme 9). Its solid-state structure has been confirmed by single-crystal X-ray analysis. The Sm^{3+} ion is η^5-bonded to the cyclopentadienyl ring, η^6-bonded to the hexagonal C_2B_4 face of $C_2B_{10}H_{11}$ cage and coordinated to two THF molecules in a distorted-tetrahedral geometry with a ring centroid–Sm–ring centroid angle of 125.1° (Fig. 15). The average Sm–cage atom and Sm–C (C_5 ring)

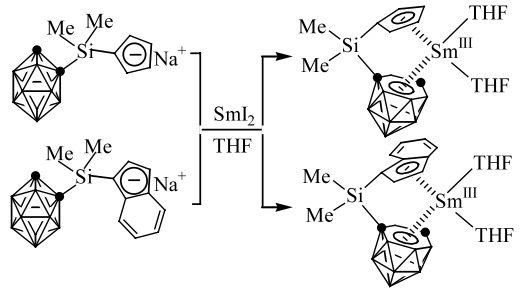

Scheme 9.

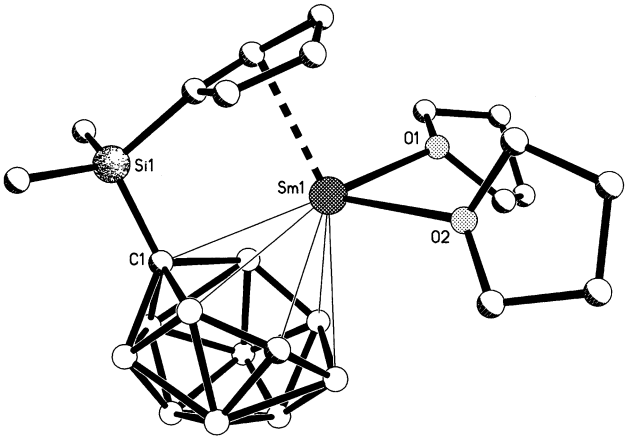

Fig. 15. Structure of $[\eta^5{:}\eta^6\text{-}Me_2Si(C_5H_4)(C_2B_{10}H_{11})]Sm(THF)_2$ [22].

distances are 2.803(3) and 2.706(2) Å, respectively. These results clearly indicate that the bridged ligand $[Me_2Si(C_5H_4)(C_2B_{10}H_{11})]^{3-}$ can indeed stabilize the mixed sandwich lanthanacarboranes and effectively prevent the ligand redistribution reactions.

Apparently, the trivalent samaracarborane $[\eta^5{:}\eta^6\text{-}Me_2Si(C_5H_4)(C_2B_{10}H_{11})]Sm(THF)_2$ is formed via an unexpected redox reaction in which Sm^{2+} is oxidized to Sm^{3+} and, meanwhile, the neutral carborane is reduced to the dianion. To further explore this new reaction, another Me_2Si-bridged ligand $Me_2Si(C_9H_7)(C_2B_{10}H_{11})$ is designed and prepared [23–25]. Interaction between SmI_2 and 1 or 2 equiv. of $[Me_2Si(C_9H_6)(C_2B_{10}H_{11})]Na$ in THF at room temperature gives the same redox product $[\eta^5{:}\eta^6\text{-}Me_2Si(C_9H_6)(C_2B_{10}H_{11})]Sm(THF)_2$ [23] (Scheme 9). Neither $[\{\eta^5\text{-}Me_2Si(C_9H_6)(C_2B_{10}H_{11})\}SmI(THF)_2]_2$ nor $[\eta^5\text{-}Me_2Si(C_9H_6)(C_2B_{10}H_{11})]_2Sm(THF)_2$ are isolated. Its solid-state structure has been confirmed by single-crystal X-ray analysis. The Sm^{3+} ion is η^5-bonded to the five-membered ring of indenyl group, η^6-bonded to the hexagonal C_2B_4 face of $C_2B_{10}H_{11}$ cage and coordinated to two THF molecules in a distorted-tetrahedral geometry with a ring centroid–Sm–ring centroid angle of 126.0° (Fig. 16). The average Sm–cage atom and Sm–C (C_5 ring) distances are 2.823(4) and 2.751(4) Å, respectively.

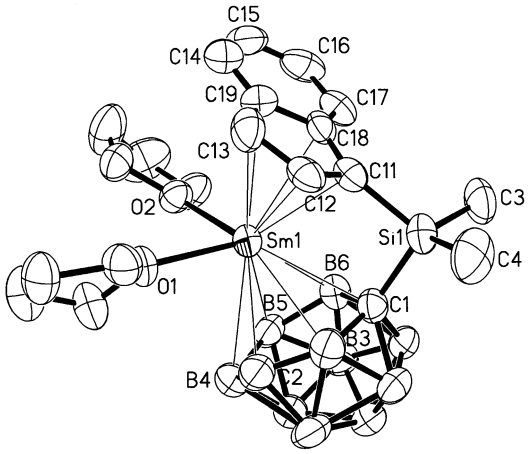

Fig. 16. Structure of $[\eta^5{:}\eta^6\text{-}Me_2Si(C_9H_6)(C_2B_{10}H_{11})]Sm(THF)_2$ [23].

To gain some insight into these unique redox reactions and reaction intermediates, a Me_2C-linked ligand $Me_2C(C_5H_5)(C_2B_{10}H_{11})$ is then developed [26,27]. Treatment of SmI_2 with 2 equiv. of $[Me_2C(C_5H_4)(C_2B_{10}H_{11})]Na(THF)$ in THF results in the isolation of both the mixed-sandwich samaracarborane $[\eta^5{:}\eta^6\text{-}Me_2C(C_5H_4)(C_2B_{10}H_{11})]Sm(THF)_2$ and the tris-ligated organosamarium compound $[\eta^5\text{-}Me_2C(C_5H_4)(C_2B_{10}H_{11})]_3Sm$ [26] (Scheme 10). The less reactive YbI_2 reacts with 2 equiv. of $[Me_2C(C_5H_4)(C_2B_{10}H_{11})]Na(THF)$ in THF to give an organoytterbium(II) compound $[\eta^5\text{-}Me_2C(C_5H_4)(C_2B_{10}H_{11})]_2Yb(THF)_2$. All these three complexes have been structurally characterized by single-crystal X-ray analyses, shown in Figs. 17–19, respectively. A possible mechanism for the formation of organosamarium complexes is then proposed and shown in Scheme 11. Interaction of SmI_2 with $[Me_2C(C_5H_4)(C_2B_{10}H_{11})]Na(THF)$ gives the first intermediate $[\eta^5\text{-}Me_2C(C_5H_4)(C_2B_{10}H_{11})]_2Sm(THF)_2$, followed by the intramolecular and then intermolecular electron transfer to generate anion $\{[\eta^5\text{-}Me_2C(C_5H_4)(C_2B_{10}H_{11})][\eta^5\text{-}Me_2C(C_5H_4)(\textit{nido}\text{-}C_2B_{10}H_{11})]Sm^{III}(THF)_2\}^-$ and cation $\{[\eta^5\text{-}Me_2C(C_5H_4)(C_2B_{10}H_{11})]_2Sm(THF)_2\}^+$. Ligand redistribution then affords the thermodynamically stable complexes $[\eta^5{:}\eta^6\text{-}Me_2C(C_5H_4)(C_2B_{10}H_{11})]Sm(THF)_2$ and $[\eta^5\text{-}Me_2C(C_5H_4)(C_2B_{10}H_{11})]_3Sm$.

Treatment of $[\eta^5\text{-}Me_2C(C_5H_4)(C_2B_{10}H_{11})]ErCl_2(THF)_3$ with 2 equiv. of Na metal or reaction of $ErCl_3$ with 1 equiv. of $[Me_2C(C_5H_4)(C_2B_{10}H_{11})]Na_3(THF)_3$ in THF at room temperature gives the same product $[\eta^5{:}\eta^6\text{-}Me_2C(C_5H_4)(C_2B_{10}H_{11})]Er(THF)_2$ [28] (Scheme 12). An X-ray analysis shows that it is isostructural with the Sm analogue. The average Er–cage atom and Er–C (C_5 ring) distances are 2.710(3) and 2.602(3) Å, respectively.

Similar salt metathesis reactions sometimes result in a slightly different product. Reaction of $[\eta^5\text{-}Me_2Si(C_9H_6)(C_2B_{10}H_{11})]ErCl_2(THF)_3$ with 2 equiv. of Na

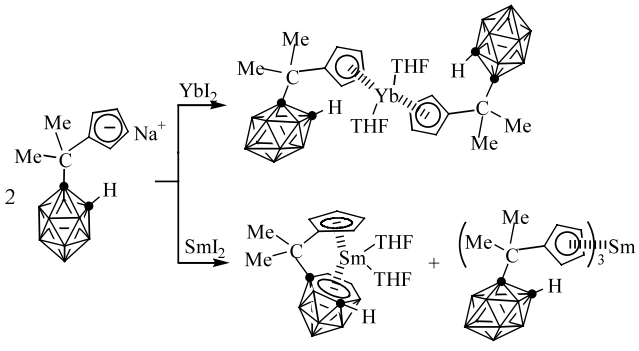

Scheme 10.

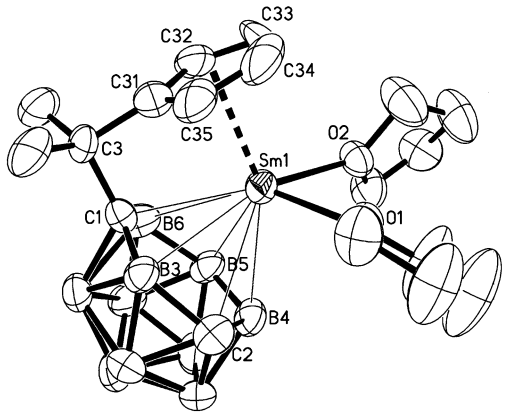

Fig. 17. Structure of $[\eta^5{:}\eta^6\text{-}Me_2C(C_5H_4)(C_2B_{10}H_{11})]Sm(THF)_2$ [26].

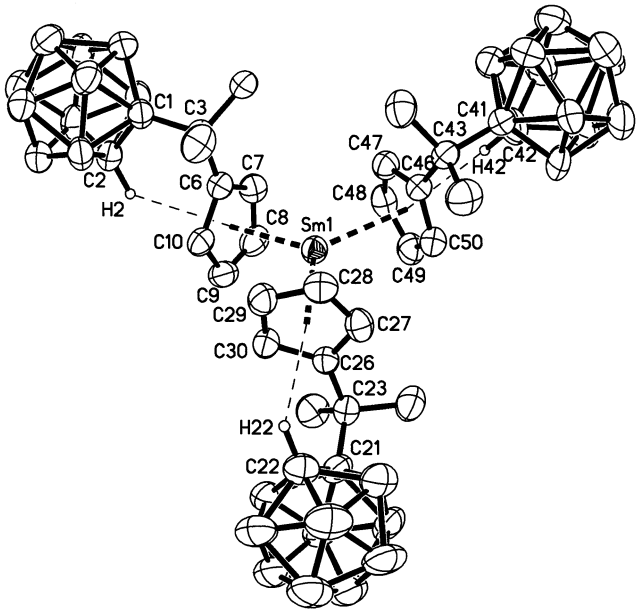

Fig. 18. Structure of $[\eta^5\text{-}Me_2C(C_5H_4)(C_2B_{10}H_{11})]_3Sm$ [26].

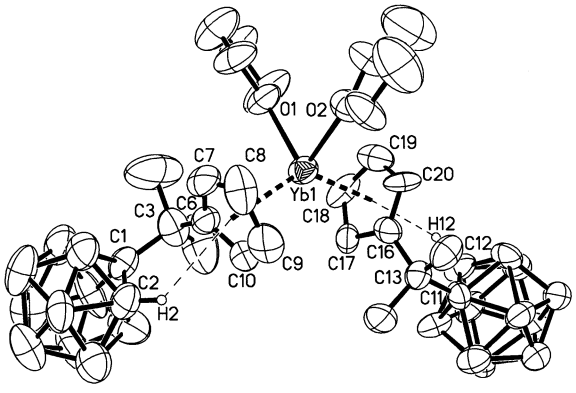

Fig. 19. Structure of $[\eta^5\text{-}Me_2C(C_5H_4)(C_2B_{10}H_{11})]_2Yb(THF)_2$ [26].

metal or reaction of $ErCl_3$ with 1 equiv. of $[Me_2Si(C_9H_6)(C_2B_{10}H_{11})]Na_3$ in THF gives the same product $[\{\eta^5{:}\eta^6\text{ - }Me_2Si(C_9H_6)(C_2B_{10}H_{11})\}Er(THF)(\mu\text{ - Cl})Na\text{-}(THF)_2]_n$ (Scheme 13). Its molecular structure has been confirmed by X-ray analyses [29]. The Er^{3+} ion is η^5-bonded to the five-membered ring of indenyl group, η^6-bonded to the hexagonal C_2B_4 face of $C_2B_{10}H_{11}$ cage and σ-bonded to a doubly bridging Cl atom and coordinated to one THF molecule in a distorted-tetrahedral geometry with a ring centroid–Er–ring

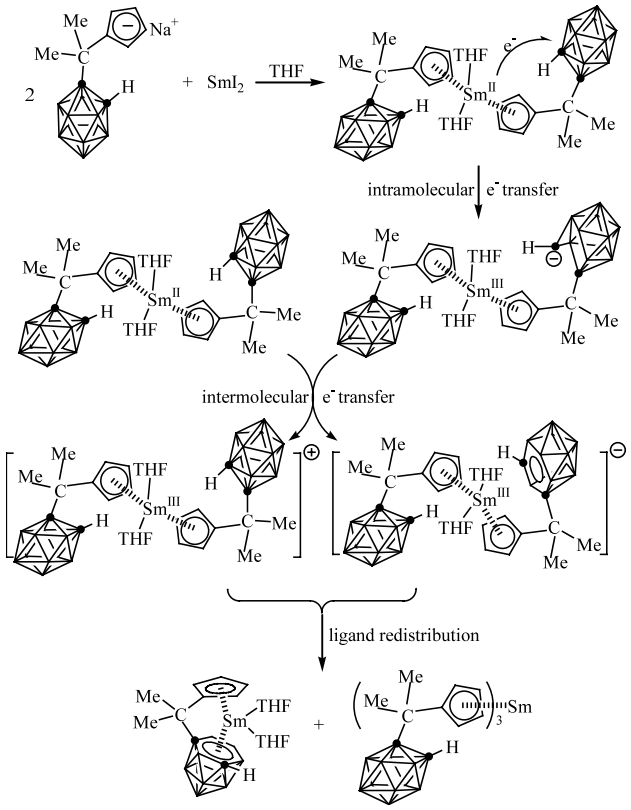

Scheme 11.

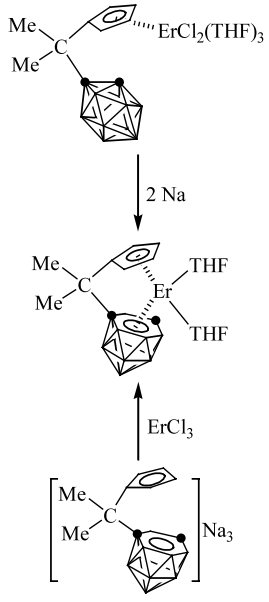

Scheme 12.

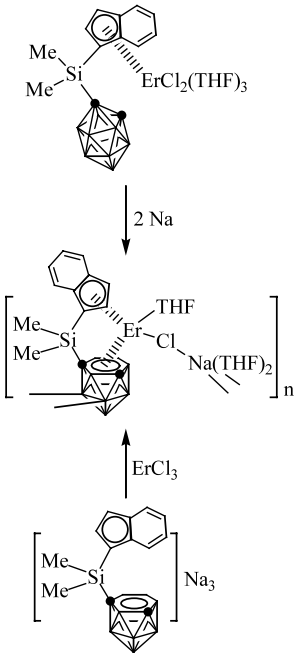

Scheme 13.

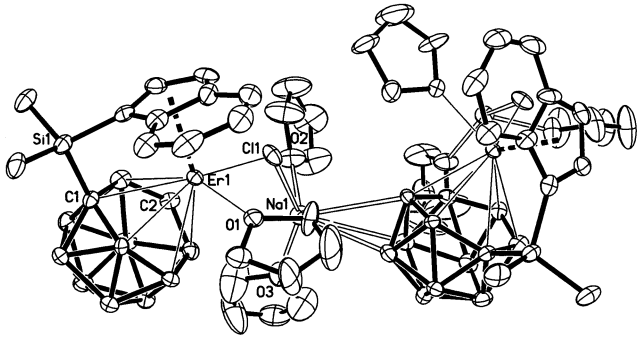

Fig. 20. Structure of $[\{\eta^5{:}\eta^6\text{-}Me_2Si(C_9H_6)(C_2B_{10}H_{11})\}Er(THF)(\mu\text{-}Cl)Na(THF)_2]_n$ [29].

centroid angle of 126.1° (Fig. 20). The average Er–cage atom and Er–C (C_5 ring) distances are 2.775(14) and 2.677(14) Å, respectively.

Sm(II) can also mediate reductive coupling of the carborane cages in certain circumstances. Treatment of $[Me_2Si(C_9H_5CH_2CH_2G)(C_2B_{10}H_{10})]Li_2(OEt_2)_2\cdot LiCl$ with 1 equiv. of $SmI_2(THF)_x$ in THF gives novel samaracarboranes $[\{\eta^5{:}\eta^1{:}\eta^6\text{-}Me_2Si(C_9H_5CH_2CH_2G)(C_2B_{10}H_{10})Sm\}_2(\mu\text{-}Cl)][Li(THF)_4]$ (G = NMe_2, OMe) as red crystals [30] (Scheme 14). X-ray analyses reveal that these two samaracarboranes have similar solid-state structures consisting of well-separated, alternating layers of discrete tetrahedral cations $[Li(THF)_4]^+$ and complex anions $[\{\eta^5{:}\eta^1{:}\eta^6\text{-}Me_2Si(C_9H_5CH_2CH_2G)(C_2B_{10}H_{10})Sm\}_2(\mu\text{-}Cl)]^-$. In the anion, each Sm^{3+} ion is η^6-bonded to *nido*-$C_2B_{10}H_{10}$ unit via a six-membered C_2B_4 bonding face, η^5-bonded to the five-membered ring of the indenyl group, and coordinated to a doubly bridging Cl atom and either the N atom or the O atom

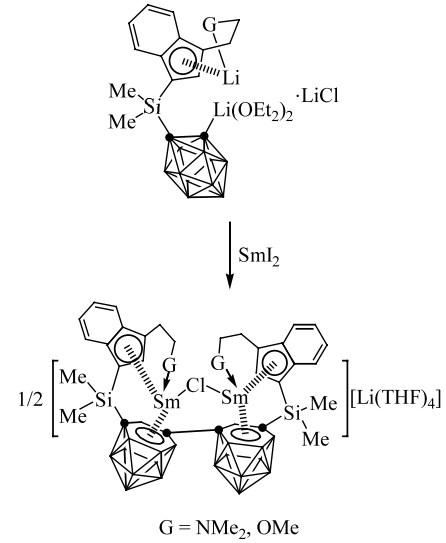

Scheme 14.

from the appended group of indenyl in a highly distorted-tetrahedral geometry with the formal coordination number of eight (Fig. 21). It is noted that two *nido*-$C_2B_{10}H_{10}$ units are connected to each other through a C–C single bond and the dihedral angles between two six-membered C_2B_4 rings are 63.3° for N-coordinated species and 69.6° for a O-coordinated one, respectively. These large angles presumably result from the steric effects. The average Sm–C(C_5 ring), Sm–cage atom and Sm–Cl(μ) distances are 2.732(8), 2.809(8) and 2.678(3) Å in N-coordinated species and 2.75(2), 2.84(3) and 2.645(4) Å in O-coordinated one, respectively. It is clear that the formation of these complexes involves two-electron reduction and coupling of the carborane cages. It may be suggested that the reaction of $SmI_2(THF)_x$ with $[Me_2Si(C_9H_5CH_2CH_2G)(C_2B_{10}H_{10})]Li_2(OEt_2)_2\cdot LiCl$ gives the first intermediate $[\eta^5{:}\eta^1{:}\sigma\text{-}Me_2Si(C_9H_5CH_2CH_2G)(C_2B_{10}H_{10})]Sm^{II}$, followed by intramolecular electron transfer from the Sm^{II} to the

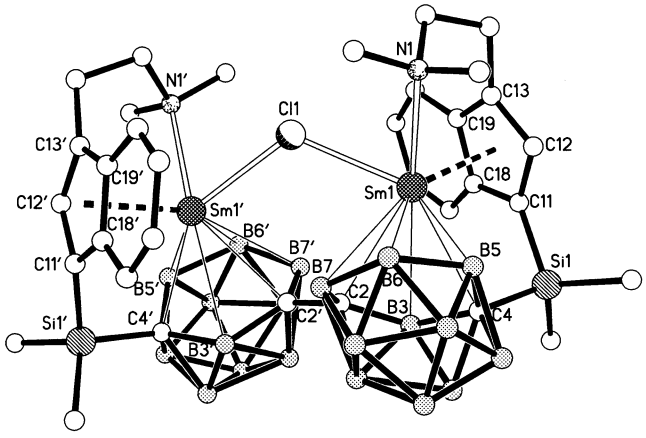

Fig. 21. Structure of $[\{\eta^5{:}\eta^1{:}\eta^6\text{-}Me_2Si(C_9H_5CH_2CH_2\text{-}NMe_2)(C_2B_{10}H_{10})Sm\}_2(\mu\text{-}Cl)]^-$ [30].

cage leading to the cleavage of the Sm–cage carbon and the cage C–C bonds; coupling of the two cages via the formation of C–C single bond generates the thermodynamically stable *nido*-species (*nido*-$RC_2B_{10}H_{10})_2^{4-}$ which then bonds to the Sm^{3+} ions in a η^6-fashion to form the final product.

All lanthanacarboranes described above incorporate 'carbons-apart' *nido*-$R_2C_2B_{10}H_{10}^{2-}$ dianions generated from two-electron reduction of *o*-$R_2C_2B_{10}H_{10}$. A novel 'carbons-adjacent' *nido*-[μ-1,2-{*o*-$C_6H_4(CH_2)_2$}-1,2-$C_2B_{10}H_{10}]^{2-}$ dianion has been discovered very recently [31,32]. Treatment of [{μ-1,2-[*o*-$C_6H_4(CH_2)_2$]-1,2-$C_2B_{10}H_{10}\}_2Na_4(THF)_6]_n$ with 2 equiv. of $ErCl_3$ in THF generates a novel half-sandwich lanthanacarborane chloride {[*o*-$C_6H_4(CH_2)_2$]$C_2B_{10}H_{10}$}$ErCl(THF)_3$ (Scheme 15). Its monomeric structure has been confirmed by an X-ray diffraction study [33]. The Er^{3+} ion is η^6-bonded to 'carbons-adjacent' *nido*-$C_2B_{10}H_{10}$ unit via a six-membered C_2B_4 bonding face, σ-bonded to a terminal Cl atom and coordinated to three THF molecules in a distorted-square-pyramidal geometry (Fig. 22). The average Er–cage atom and Er–Cl distances are 2.769(15) and 2.544(4) Å, respectively. It is expected that a novel class of lanthanacarboranes incorporating 'carbons-adjacent' *nido*-$R_2C_2B_{10}H_{12}^{2-}$ ligands will be generated in the near future.

2.2.2. *arachno*-C_2B_{10} systems

According to electron-counting rules, *o*-$R_2C_2B_{10}H_{10}$ can accept four electrons to give *arachno*-$R_2C_2B_{10}H_{10}^{4-}$ tetraanions [34]. The only metallacarborane bearing the

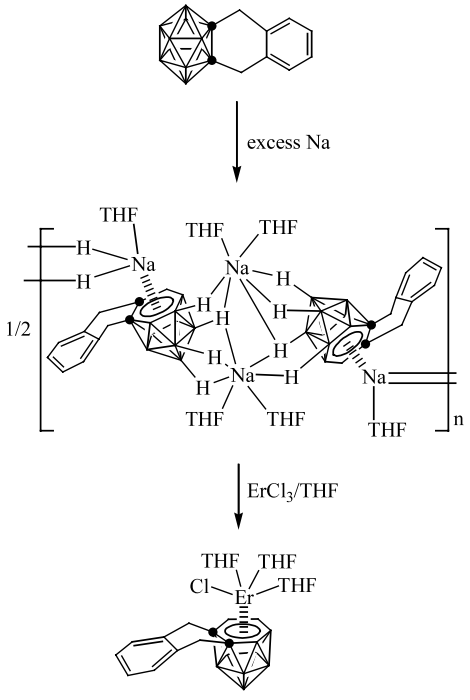

Scheme 15.

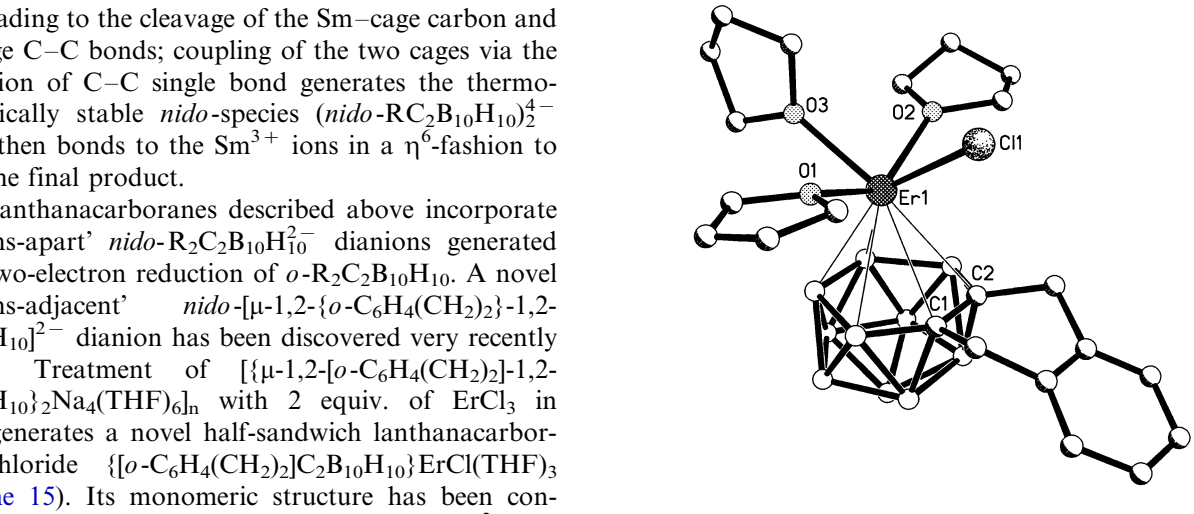

Fig. 22. Structure of {[*o*-$C_6H_4(CH_2)_2$]$C_2B_{10}H_{10}$}$ErCl(THF)_3$ [33].

arachno-$R_2C_2B_{10}H_{10}^{4-}$ ligand is (η^6:η^6-$C_2B_{10}H_{12}$)-[$Co(\eta^5$-$C_5H_5)]_2$ with the proposed geometry of a bicapped hexagonal antiprism [35].

Reaction of [η^5-$Me_2C(C_5H_4)(C_2B_{10}H_{11})$]$LnCl_2$-$(THF)_3$ or [η^5:η^6-$Me_2C(C_5H_4)(C_2B_{10}H_{11})$]$Ln(THF)_2$ with excess Na metal in THF at room temperature affords the same products, namely novel 13-vertex lanthanacarboranes [{[η^5:η^7-$Me_2C(C_5H_4)(C_2B_{10}$-$H_{11})$]Ln$\}_2\{Na_4(THF)_9\}]_n$ (Ln = Dy, Er) [26,28] (Scheme 16). Their polymeric nature has been confirmed by an X-ray diffraction study. Each asymmetrical unit contains two [η^5:η^7-$Me_2C(C_5H_4)(C_2B_{10}H_{11})$]$Er^{2-}$ structural motifs that are connected by three Na atoms through several B–H–Na two-electron-three-center (2e–3c) bonds (Fig. 23). The asymmetrical units are

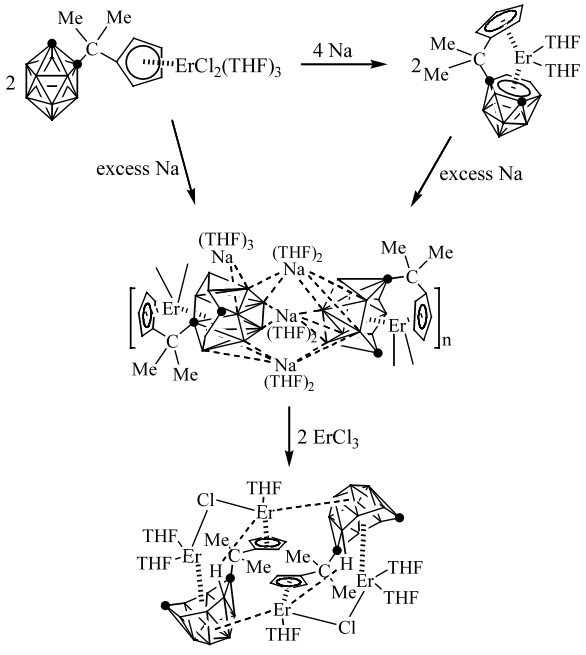

Scheme 16.

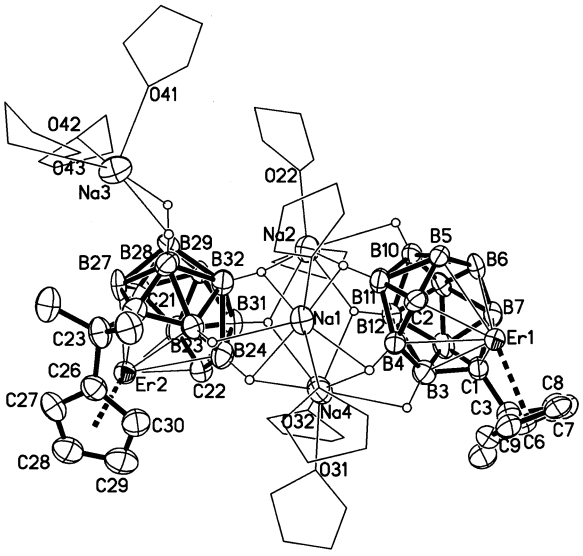

Fig. 23. Structure of $[\{\eta^5{:}\eta^7\text{-}Me_2C(C_5H_4)(C_2B_{10}H_{11})\}Er]_2\{Na_4(THF)_9\}]_n$ [28].

then linked to each other via B–H–Er bonds to form an infinitive polymeric chain. Each Er^{3+} ion is η^7-bonded to $[arachno\text{-}C_2B_{10}H_{11}]^{4-}$, η^5-bonded to cyclopentadienyl, and σ-bonded to two B–H bonds from the neighboring $[arachno\text{-}C_2B_{10}H_{11}]^{4-}$ unit in a distorted-tetrahedral arrangement. The carborane ligand $[arachno\text{-}C_2B_{10}H_{11}]^{4-}$ has a boat-like C_2B_5 bonding face in which the five B atoms are coplanar and the two C atoms are ca. 0.6 Å above this plane, resulting in an average Er–C(cage) distance being ca. 0.26 Å shorter than the average Er–B(cage) distance (Fig. 24). This is the first lanthanacarborane containing a η^7-carboranyl ligand.

The Na^+ ions in these complexes can be completely replaced by other ions. For example, treatment of $[\{[\eta^5{:}\eta^7\text{-}Me_2C(C_5H_4)(C_2B_{10}H_{11})]Er\}_2\{Na_4(THF)_9\}]_n$ with 2 equiv. of $ErCl_3$ in THF at room temperature

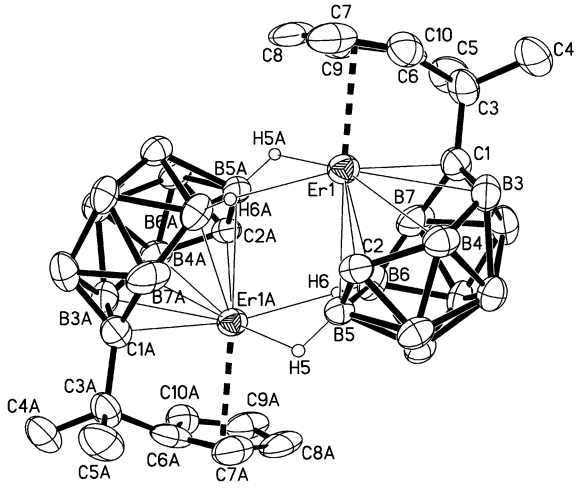

Fig. 24. Interactions between two asymmetric units.

gives a novel tetranuclear metallacarborane cluster $[\{\eta^5{:}\eta^7\text{-}Me_2C(C_5H_4)(C_2B_{10}H_{11})\}Er_2(\mu\text{-}Cl)(THF)_3]_2$ [28] (Scheme 16). It is noteworthy that the added Er^{3+} ions not only replace the Na^+ ions but also compete with the existing Er^{3+} ions for the coordination sites, resulting in the formation of a new structural motif, which offers an opportunity to prepare heteronuclear metallacarboranes. The solid-state structure shows that it is a centrosymmetric tetranuclear metallacarborane cluster with two $\{[\eta^5{:}\eta^7\text{-}Me_2C(C_5H_4)(C_2B_{10}H_{11})]Er_2(\mu\text{-}Cl)(THF)_3\}$ units that are connected by two sets of three B–H–Er 2e–3c bonds (Fig. 25). Each of the two Er(1) atoms is η^7-bonded to $[arachno\text{-}C_2B_{10}H_{11}]^{4-}$ and coordinated to two O atoms from THF molecules and one doubly bridging Cl atom in a distorted-tetrahedral geometry, a structure motif which differs significantly from that of $[\{[\eta^5{:}\eta^7\text{-}Me_2C(C_5H_4)(C_2B_{10}H_{11})]Er\}_2\{Na_4(THF)_9\}]_n$. Each of the other two Er(2) atoms is η^5-bonded to the cyclopentadienyl ring and coordinated to one O atom from the THF molecule, one B–H bond from $[arachno\text{-}C_2B_{10}H_{11}]^{4-}$, one doubly bridging Cl atom, and three B–H bonds from the neighboring $[arachno\text{-}C_2B_{10}H_{11}]^{4-}$ ligand in a distorted-pentagonal-bipyramidal geometry with the centroid of the cyclopentadienyl ring and H(9A) occupying the axial sites. The average Er(2)–C(C_5 ring) distance of 2.597(4) Å, Er(1)–B(cage) distance of 2.655(7) Å and Er···B interatomic distance of 2.787(4) Å are all shorter than the corresponding values in $[\{[\eta^5{:}\eta^7\text{-}Me_2C(C_5H_4)(C_2B_{10}H_{11})]Er\}_2\{Na_4(THF)_9\}]_n$, perhaps due to steric reasons.

The η^7 is a completely new bonding mode for carborane molecules and represents the highest hapticity of carboranyl ligands ever reported in the literature. To explore the generality of this bonding mode and to

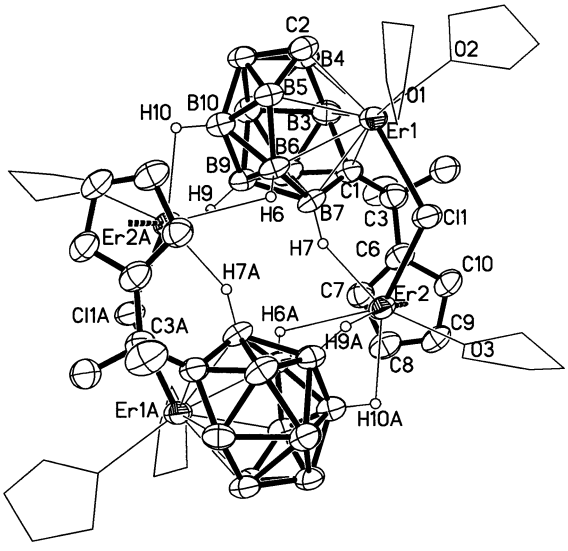

Fig. 25. Structure of $[\{\eta^5{:}\eta^7\text{-}Me_2C(C_5H_4)(C_2B_{10}H_{11})\}Er_2(\mu\text{-}Cl)(THF)_3]_2$ [28].

better understand the bonding interactions between metal ion and η^7-carborane anion, several lanthanacarboranes of the general formula $\{\eta^7$-$[(C_6H_5CH_2)_2$-$C_2B_{10}H_{10}]Ln(THF)\}_2\{Na(THF)_3\}_2$ (Ln = Dy, Y, Er) are prepared by treatment of 1,2-$(C_6H_5CH_2)_2$-1,2-$C_2B_{10}H_{10}$ with excess Na metal in THF, followed by reaction with 1 equiv. of $LnCl_3$ in the presence of excess Na metal at reflux temperature [36]. The coordinated THF molecules in these lanthanacarboranes can be replaced by DME molecules giving $\{\eta^7$-$[(C_6H_5CH_2)_2$-$C_2B_{10}H_{10}]Ln(DME)\}_2\{Na(DME)_2\}_2$ after recrystallization from a DME solution. Reaction of 1,2-$(C_6H_5CH_2)_2$-1,2-$C_2B_{10}H_{10}$ with excess Li metal, followed by reaction with 2 equiv. of $LnCl_3$ at room temperature gives $[\eta^7$-$\{(C_6H_5CH_2)_2C_2B_{10}H_{10}\}$-$Ln(THF)]_2[Li(THF)_4]_2$ (Ln = Y, Er) (Scheme 17). Since 1,2-$(C_6H_5CH_2)_2$-1,2-$C_2B_{10}H_{10}$ cannot be directly converted into the [*arachno*-$(C_6H_5CH_2)_2C_2B_{10}H_{10}]^{4-}$ by either Li or Na metal, it is reasonable to suggest that the 13-vertex *closo*-metallacarborane $[\eta^6$-$(C_6H_5CH_2)_2$-$C_2B_{10}H_{10}]MCl(THF)_x$ may serve as an intermediate which accepts two more electrons from Na metal to form the final product.

These lanthanacarboranes are fully characterized by various spectroscopic data and X-ray analyses. Figs. 26 and 27 show the representative structures of THF- and DME-coordinated species, respectively. Each central metal ion is η^7-bonded to the [*arachno*-$(C_6H_5CH_2)_2C_2B_{10}H_{10}]^{4-}$ tetraanion and σ-bonded to two B–H bonds from the neighboring [*arachno*-

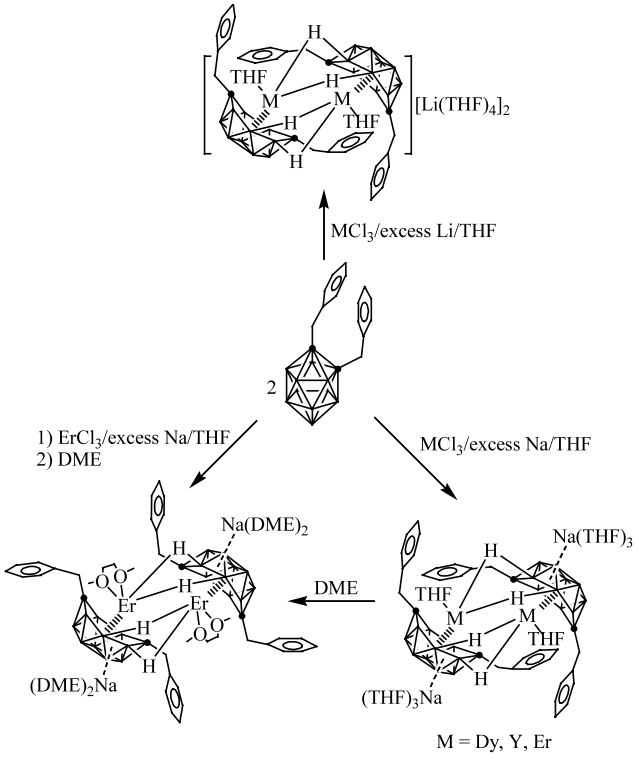

Scheme 17.

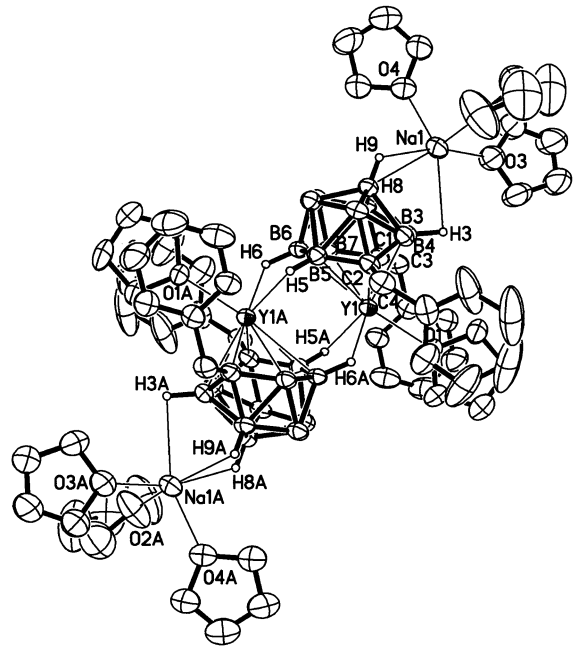

Fig. 26. Structure of $\{\eta^7$-$[(C_6H_5CH_2)_2C_2B_{10}H_{10}]Y(THF)\}_2\{Na$-$(THF)_3\}_2$ [36].

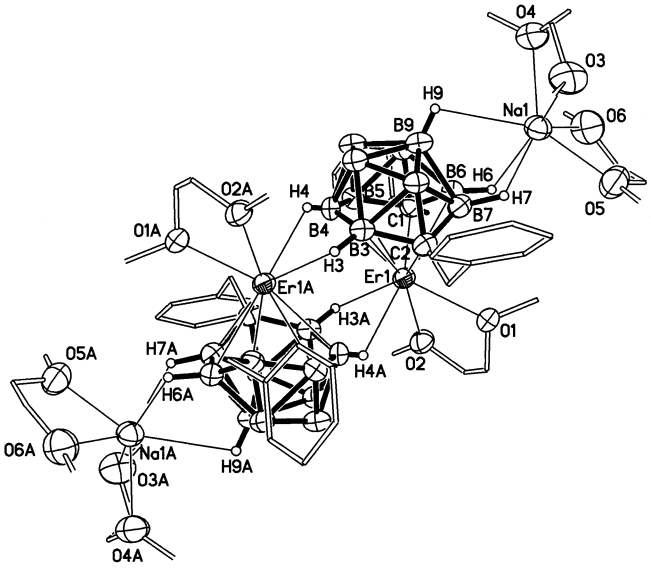

Fig. 27. Structure of $\{\eta^7$-$[(C_6H_5CH_2)_2C_2B_{10}H_{10}]Er(DME)\}_2\{Na$-$(DME)_2\}_2$ [36].

$(C_6H_5CH_2)_2C_2B_{10}H_{10}]^{4-}$ ligand and either one oxygen atom of THF molecule or two oxygen atoms of DME molecule. The closest approach of Ln^{3+} to benzyl groups is greater than 3.7 Å, which indicates there are no obvious interactions between Ln^{3+} and benzyl substituents. Like the carboranyl ligand in $[\{[\eta^5$:η^7-$Me_2C(C_5H_4)(C_2B_{10}H_{11})]Er\}_2\{Na_4(THF)_9\}]_n$ [28], the [*arachno*-$(C_6H_5CH_2)_2C_2B_{10}H_{10}]^{4-}$ has a boat-like C_2B_5 bonding face in which the five B atoms are coplanar and the two C atoms are ca. 0.6 Å above this

plane, leading to three different types of coordination environment for cage atoms: 5-coordinate carbon, 6-coordinate boron, and 7-coordinate boron, respectively. It is noted that the average Ln–C(cage) distances in these lanthanacarboranes are all at the short end of the relevant Ln–C σ bond distances found in organolanthanide complexes.

The above results show that the arrangement of the cage atoms in [*arachno*-$R_2C_2B_{10}H_{10}]^{4-}$ is the same regardless of the substituents on the cage carbons and the d^0/f^n transition metal ions. To understand the bonding interactions between the metal ion and the *arachno*-carboranyl ligand, molecular orbital calculations have been performed on the yttrium analogue. The results indicate that the five d orbitals of Y are all significantly involved in the metal-[η^7-$C_2B_{10}H_{12}$] bonding interactions. A schematic molecular orbital interaction diagram can be derived, shown in Fig. 28. The natural bond order (NBO) analysis of [*arachno*-$C_2B_{10}H_{12}]^{4-}$ shows that in the boat-like C_2B_5 bonding face the natural atomic charges of carbons (av. −0.85) are significantly higher than those of borons (av. −0.16), implying that the carbons should form stronger bonds with the metal center. These results are in good agreement with the experimental data. On the basis of molecular orbital calculations, it is anticipated that (1) only d^0 and f-block transition metal ions with proper size can have such bonding interactions with [*arachno*-$C_2B_{10}H_{12}]^{4-}$ ligand and (2) only f-block transition metal ions can form full-sandwich metallacarboranes with [*arachno*-$C_2B_{10}H_{12}]^{4-}$ ligands since they do not obey the 18-electron rule.

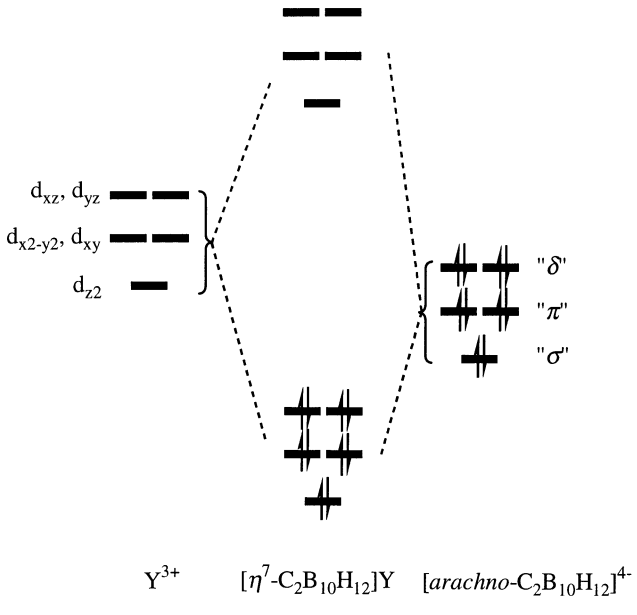

Fig. 28. Schematic orbital interaction diagram showing the interactions between Y^{3+} and the *arachno*-$C_2B_{10}H_{12}^{4-}$ cage fragment.

Interaction between $YbCl_3$, 1 equiv. of [Me_2-$Si(C_{13}H_8)(C_2B_{10}H_{11})$]$Li(OEt_2)_2$ and excess finely cut Na metal in THF at room temperature followed by treatment with 1 equiv. of dry Me_3NHCl gives a novel full-sandwich lanthanacarborane complex {{[η^7-Me_2-$Si(C_{13}H_9)(C_2B_{10}H_{11})$]$_2Yb^{III}$}$_2Yb^{II}$}{$Na_8(THF)_{20}$} [37] (Scheme 18). An X-ray diffraction study reveals that it is a novel centrosymmetric mixed valence complex with the Yb^{II} sitting at an inversion center. Two full-sandwich metallacarboranes that are connected by a Yb^{2+} ion through four sets of two B–H–Yb bonds form the core structure of the complex (Fig. 29). The charge is then compensated by complexation with eight $Na(THF)_n^+$ complex ions via many B–H–Na bonds, resulting in a nicely packed structure. These surrounding complex ions protect the Yb^{II} from the attack of Me_3NH^+ stabilizing the very unusual $Yb^{II}(H–B)_8$ unit. It is well-documented that organoytterbium(III) compounds can be readily reduced by Na metal to form the Yb^{II} species [4]. Complex {{[η^7-Me_2-$Si(C_{13}H_9)(C_2B_{10}H_{11})$]$_2Yb^{III}$}$_2Yb^{II}$}{$Na_8(THF)_{20}$} is an exceptional example in which the capping Yb^{III} remains intact in the presence of excess Na metal, suggesting that the *arachno*-$R_2C_2B_{10}H_{10}^{4-}$ tetraanion can effectively stabilize high oxidation states of the metals. Each Yb^{3+} ion is η^7-bonded to two *arachno*-carboranyl ligands in a bent sandwich structure with the ring centroid–Yb–ring centroid angle of 160.2°. The average Yb(III)–C(cage) and Yb(III)–B(cage) distances are 2.451(4) and 2.771(4) Å, respectively.

2.3. C_2B_4 systems

The C_2B_4 ligand system was introduced to lanthanide chemistry in 1992 by Hosmane [38]. Treatment of $LnCl_3$ with 2 equiv. of [$(Me_3Si)_2C_2B_4H_4$]$Li_2(THF)_4$ in benzene gives half-sandwich lanthanacarborane clusters [{η^5-

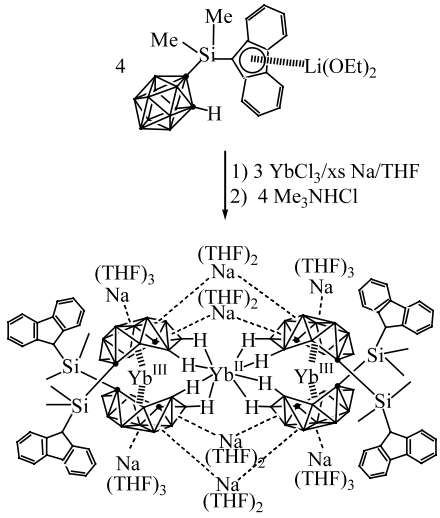

Scheme 18.

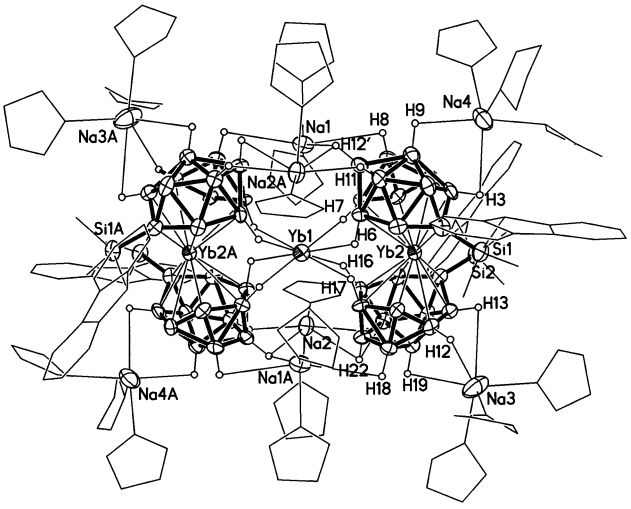

Fig. 29. Structure of $\{\{[\eta^7\text{-}Me_2Si(C_{13}H_9)(C_2B_{10}H_{11})]_2Yb^{III}\}_2Yb^{II}\}\text{-}\{Na_8(THF)_{20}\}$ [37].

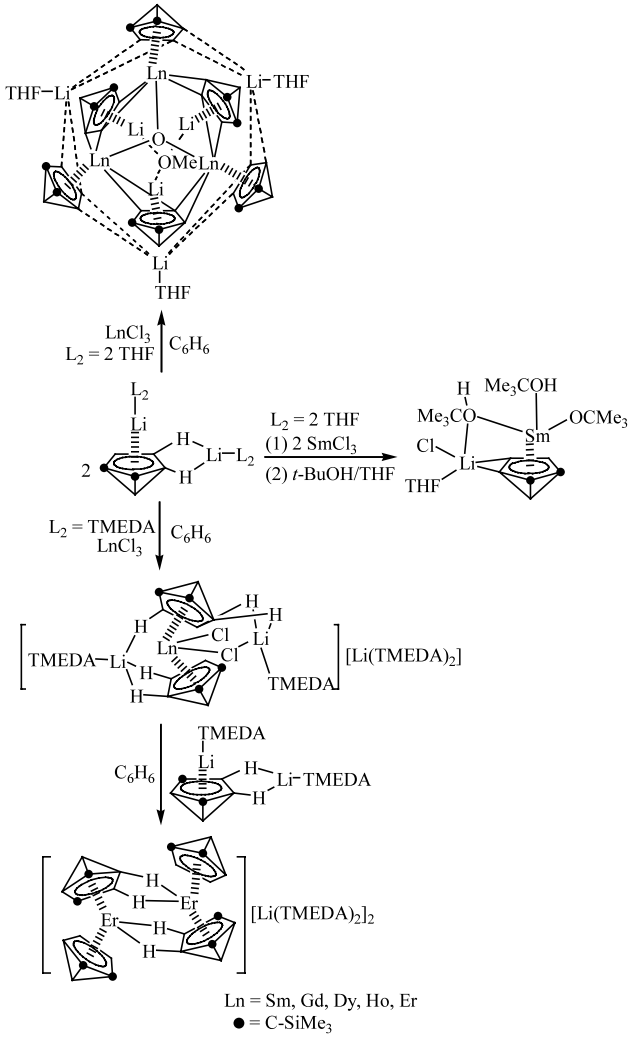

Scheme 19.

$[(Me_3Si)_2C_2B_4H_4]Ln\}_3][\{((Me_3Si)_2C_2B_4H_4)Li\}_3(\mu_3\text{-}OMe)][Li(THF)]_3(\mu_2\text{-}O)$ (Ln = Sm, Gd, Tb, Dy, Ho) [38–40] (Scheme 19). Since THF is the only oxygen-containing substance in the synthetic scheme, it is believed that THF is the oxygen source for the oxyanions in the products. These oxyanions stabilize the cluster of the half-sandwich complexes to the extent that the lanthanacarborane syntheses are effectively terminated at that stage. Their structures have been confirmed by single-crystal X-ray analyses. They are all isostructural and isomorphous. A representative structure is shown in Fig. 30. It consists of three half-sandwich lithiacarboranes and three half-sandwich lanthanacarboranes arranged around a methoxide ion and an oxide ion, respectively. The Ln_3O geometry is that of a trigonal plane in which the three lanthanides equally surround the central oxide. It is noted that these lanthanacarborane clusters are unreactive toward either additional $LnCl_3$ or dilithiacarborane.

An equimolar reaction between $SmCl_3$ and $[(Me_3Si)_2C_2B_4H_4]Li_2(THF)_2$ in benzene followed by treatment with a mixture of *t*-BuOH/THF/hexane gives a monomeric half-sandwich samaracarborane $\{[\eta^5\text{-}(Me_3Si)_2C_2B_4H_4]Sm(OBu^t)(Bu^tOH)_2\}\{LiCl(THF)\}$ [41] (Scheme 19). An X-ray analysis reveals that the Sm^{3+} ion is η^5-bonded to one carboranyl ligand and σ-bonded to three oxygen atoms from Bu^tO^- monoanion and Bu^tOH, respectively, in a distorted-tetrahedral geometry (Fig. 31). The average Sm–cage atom distance is 2.794(9) Å. The Sm–O(18) (Bu^tO) distance of 2.101(6)

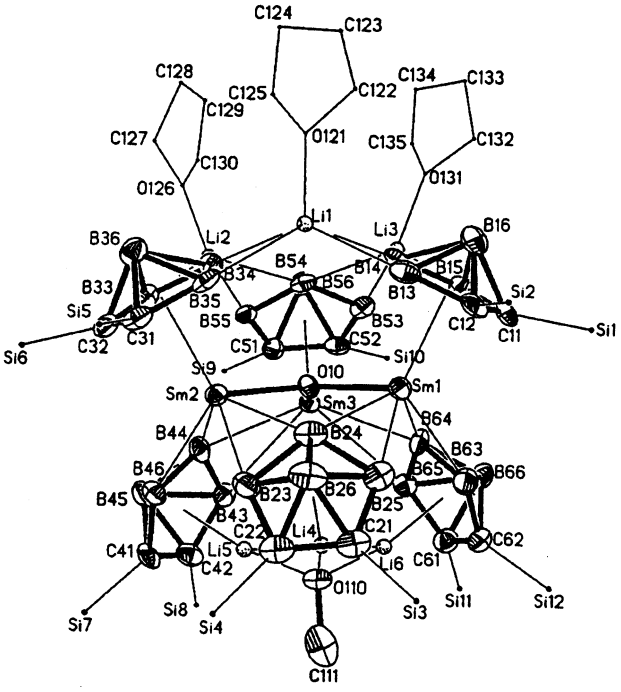

Fig. 30. Structure of $[\{\eta^5\text{-}[(Me_3Si)_2C_2B_4H_4]Sm\}_3][\{((Me_3Si)_2C_2B_4H_4)Li\}_3(\mu_3\text{-}OMe)][Li(THF)]_3(\mu_2\text{-}O)$ [40].

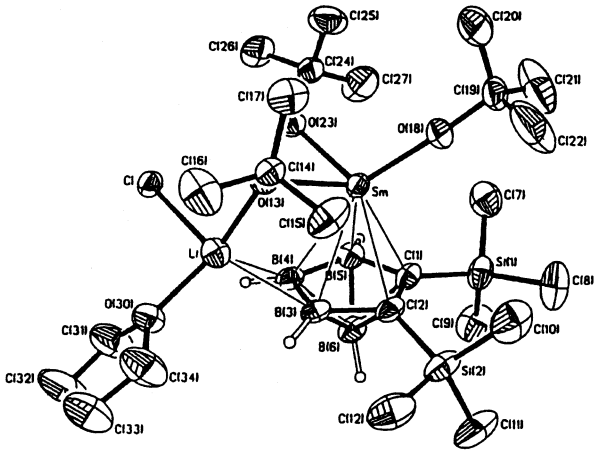

Fig. 31. Structure of $\{[\eta^5\text{-}(Me_3Si)_2C_2B_4H_4]Sm(OBu^t)(Bu^tOH)_2\}\text{-}\{LiCl(THF)\}$ [41].

Å is significantly shorter than the Sm–O(13,23) (Bu^tOH) distances of 2.310(5) and 2.308(5) Å. The C(19)–O(18)–Sm angle of 177.7(5)° is significantly larger than other two C–O–Sm angles (117.7(5) and 126.0(5)°), which may indicate there are some multiple bondings between Sm and O(18).

To gain some insight into the above reactions, a TMEDA-solvated dilithiacarborane (TMEDA = tetramethylethylenediamine) is used to replace the THF-solvated one; reaction of $LnCl_3$ with 2 equiv. of $[(Me_3Si)_2C_2B_4H_4]Li_2(TMEDA)_2$ in benzene affords expected full-sandwich lanthanacarboranes $[\{\eta^5\text{-}(Me_3Si)_2C_2B_4H_4\}_2LnCl_2][Li_3(TMEDA)_4]$ (Ln = Sm, Gd, Dy, Ho, Er) [42] (Scheme 19). These results indicate that (1) in the absence of THF molecules, the reactions lead to the formation of the expected full-sandwich lanthanacarboranes and (2) the oxide ions are likely produced by the degradation of the THF molecules, which stabilizes the clusters of the half-sandwich complexes. These complexes are fully characterized by various spectroscopic data and X-ray analyses. Fig. 32 shows their representative structure. The Ln^{3+} ion is η^5-bonded to each of two carboranyl ligands and σ-bonded to two chloro atoms in a distorted-tetrahedral geometry. The ring centroid–Ln–ring centroid angles are 117.3° for Sm and 128.6 ± 0.6° for the other three complexes. The average Ln–cage atom distances are very similar to the corresponding values found in the previously mentioned trinuclear clusters of these metals. The Ln–Cl(μ) distance is about 0.5 Å longer than the corresponding Ln–Cl(terminal) length, except the Sm analogue in which the Sm–Cl(terminal) distance is unusually longer than the Sm–Cl(μ) one.

The two chloro groups in the above complexes are reactive and can be replaced by other π ligands. For example, treatment of $[\{\eta^5\text{-}(Me_3Si)_2C_2B_4H_4\}_2ErCl_2]\text{-}[Li_3(TMEDA)_4]$ with an equimolar amount of TMEDA-solvated 'carbons-apart' dilithiacarborane $[2,4\text{-}(Me_3Si)_2C_2B_4H_4]Li_2(TMEDA)_2$ in benzene produces a mixed-carborane sandwich complex $[\{(\eta^5\text{-}2,3\text{-}(Me_3Si)_2C_2B_4H_4)(\eta^5\text{-}2,4\text{-}(Me_3Si)_2C_2B_4H_4)Er\}_2][Li(TMEDA)_2]_2$ [43] (Scheme 19). This reaction involves the substitution of one of the complexed 2,3-C_2B_4 units by a 2,4-C_2B_4 ligand, along with concomitant Cl^- elimination and dimerization of the resulting erbacarborane mixed-sandwich complexes. Its molecular structure is shown in Fig. 33. Each Er^{3+} ion is η^5-bonded to one

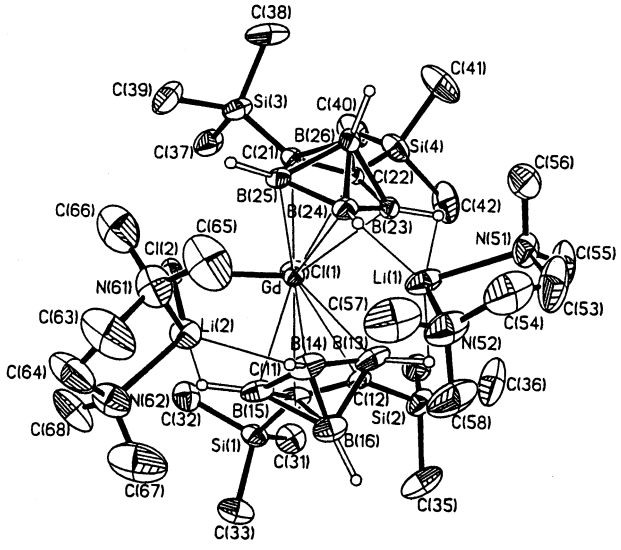

Fig. 32. Structure of $[\{[\eta^5\text{-}(Me_3Si)_2C_2B_4H_4]_2GdCl_2\}\{Li(TMEDA)\}_2]^-$ [42].

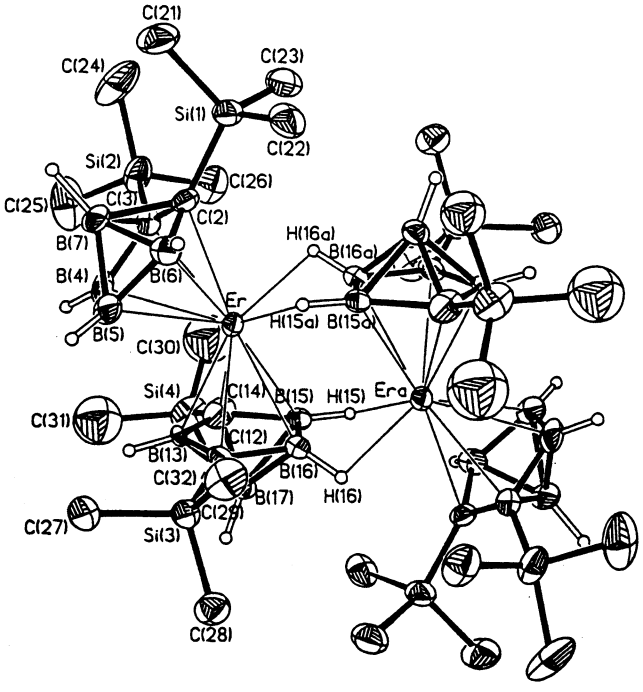

Fig. 33. Structure of $[\{(\eta^5\text{-}2,3\text{-}(Me_3Si)_2C_2B_4H_4)(\eta^5\text{-}2,4\text{-}(Me_3Si)_2\text{-}C_2B_4H_4)Er\}_2]^{2-}$ [43].

2,3-C_2B_4 and one 2,4-C_2B_4 ligands and σ-bonded to one neighboring 2,4-C_2B_4 unit via two Er–H–B bonds in a highly distorted-tetrahedral geometry with a ring centroid–Er–ring centroid angle of 135.5°. The average Er–cage atom (2,4-C_2B_4) distance is longer than the corresponding value to 2,3-C_2B_4 unit.

Surprisingly, an equimolar reaction between $HoCl_3$ and a TMEDA-solvated 'carbons-apart' dilithiacarborane [2,4-$(Me_3Si)_2C_2B_4H_4$]Li_2(TMEDA)$_2$ in benzene also gives the full-sandwich lanthanacarborane {[η^5-2,4-$(Me_3Si)_2C_2B_4H_4]_2HoCl_2$}{$HoCl_2$(TMEDA)}{$Li_2$(TMEDA)$_2$} [44] (Scheme 20). Its molecular structure has been confirmed by single-crystal X-ray analysis. As shown in Fig. 34, the central Ho atom is η^5-bonded to each of two carboranyl ligands and σ-bonded to two doubly bridging Cl atoms in a distorted-tetrahedral geometry with a ring centroid–Ho–ring centroid angle of 130.2°. The other Ho atom is σ-bonded to each of two carboranyl ligands via one set of two Ho–H–B bonds, two doubly bridging Cl atoms and coordinated to one TMEDA molecule. The average Ho–cage atom and Ho···B distances are 2.701(10) and 2.690(10) Å, respectively. The mechanism for this reaction is not known.

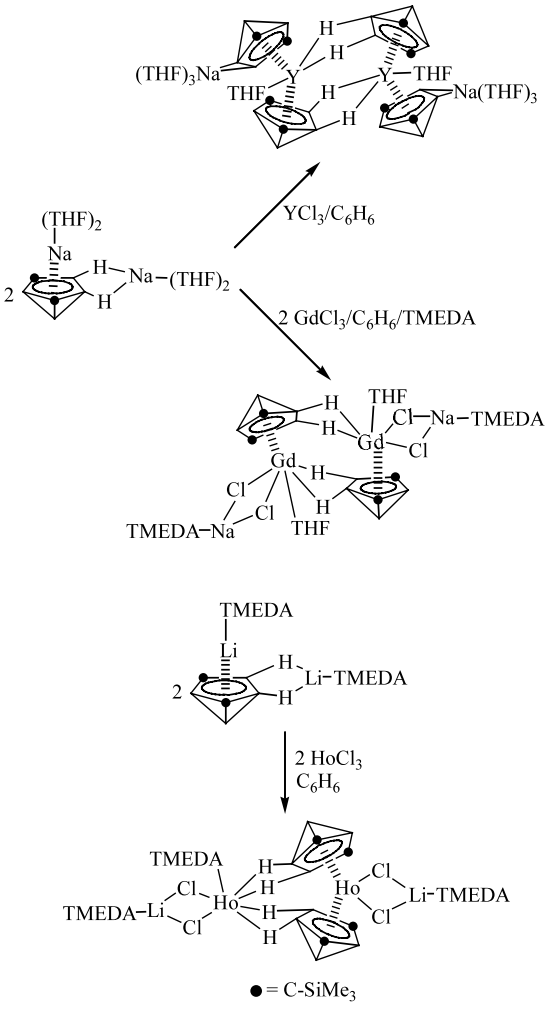

Scheme 20.

On the other hand, interaction between $GdCl_3$ and a THF-solvated 'carbons-apart' dinatracarborane [2,4-$(Me_3Si)_2C_2B_4H_4]Na_2(THF)_4$ in benzene generates a half-sandwich lanthanacarborane dimer [{η^5-2,4-$(Me_3Si)_2C_2B_4H_4$}Gd(THF)(μ-Cl)$_2$Na(TMEDA)]$_2$ [45] (Scheme 20). Fig. 35 shows its solid-state structure. Each Gd^{3+} ion is η^5-bonded to one carboranyl ligand, σ-bonded to two doubly bridging Cl atoms and the neighboring carborane cage via one set of two Gd–H–B bonds and coordinated to one THF molecule in a distorted-octahedral geometry. The average Gd–cage atom and Gd–Cl distances are 2.725(13) and 2.669(3) Å, respectively.

The chemistry of yttrium is very similar to that of the lanthanides and is often included with them. However, exceptional examples of yttrium compounds not analogous to lanthanide compounds can sometimes be found. Treatment of YCl_3 with 2 equiv. of [2,3-$(Me_3Si)RC_2B_4H_4]Li_2(THF)_4$ in benzene gives full-sandwich yttracarboranes {[η^5-2,3-$(Me_3Si)RC_2B_4H_4]_2YCl$(THF)}{$Li_2(THF)_5$} (R = Me_3Si, Me) which can further react with excess NaH affording the corresponding metal hydride species formulated as [{[η^5-2,3-$(Me_3Si)_2C_2B_4H_4]_2Y(\mu$-H)}{$Li_2(THF)_2$}]$_2$ [46] (Scheme 21). In comparison with the lanthanacarborane clusters described in Scheme 19, it is surprising that similar reactions offer very different products. On the other hand, reaction of YCl_3 with 2 equiv. of 'carbons-apart' [2,4-$(Me_3Si)_2C_2B_4H_4]Na_2(THF)_4$ in benzene/THF affords a full-sandwich yttracarborane dimer [{[η^5-2,4-$(Me_3Si)_2C_2B_4H_4]_2Y$}{$Na(THF)_3$}]$_2$ (Scheme 20). The driving force for the dimerization may be due to relief of steric strains in going from the 'carbons-adjacent' to the 'carbons-apart' carborane cages. Direct substitution of the chloro group in {[η^5-2,3-$(Me_3Si)_2C_2B_4H_4]_2YCl$(THF)}{$Li_2(THF)_5$} by an alkyl unit is unsuccessful. An attempted synthesis of such a complex by an initial reaction of YCl_3 with Me_3SiCH_2MgCl, followed by reaction with the neutral carborane 2,3-$(Me_3Si)_2C_2B_4H_6$ in a 1:2 molar ratio produces an unexpected mixed magnesa-/yttracarborane {[η^5-2,3-$(Me_3Si)_2C_2B_4H_4]Y(\mu$-$Cl)_3$}{[$\eta^5$-2,3-$(Me_3Si)_2C_2B_4H_4$]Mg(THF)}{$Mg(THF)_2$} (Scheme 21). It is not known if the Cl ions came from the YCl_3 or the Grignard reagent. High solubility of $MgCl_2$ in THF may be responsible for the formation of such a high chloro ion-containing complex.

Figs. 36–38 show the solid-state structures of {[η^5-2,3-$(Me_3Si)_2C_2B_4H_4]_2YCl$ (THF)}{$Li_2(THF)_5$}, [{[η^5-2,4-$(Me_3Si)_2C_2B_4H_4]_2Y$}{$Na(THF)_3$}]$_2$ and {[η^5-2,3-$(Me_3Si)_2C_2B_4H_4]Y(\mu$-Cl)$_3$}{[$\eta^5$-2,3-$(Me_3Si)_2C_2B_4H_4$]-Mg(THF)}{$Mg(THF)_2$}, respectively. The bonding interactions between metal ions and carboranyl ligands

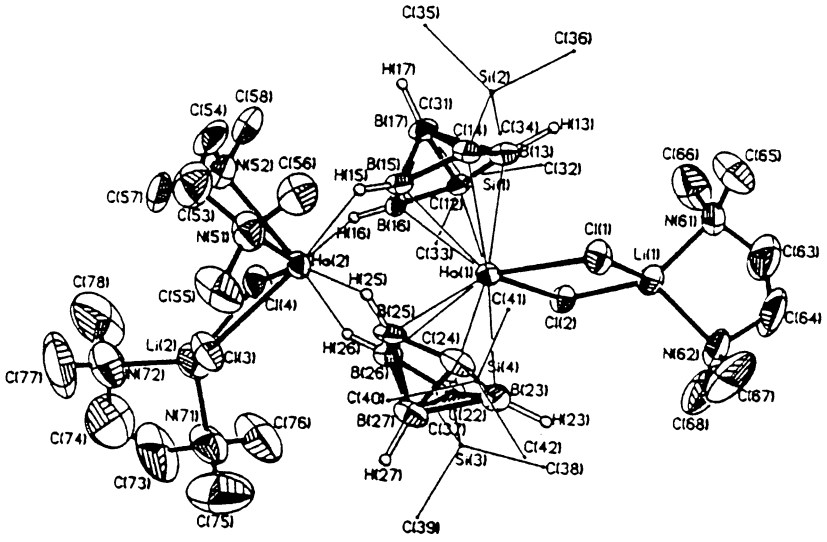

Fig. 34. Structure of $\{[\eta^5\text{-}2,4\text{-}(Me_3Si)_2C_2B_4H_4]_2HoCl_2\}\{HoCl_2(TMEDA)\}\{Li(TMEDA)\}_2$ [44].

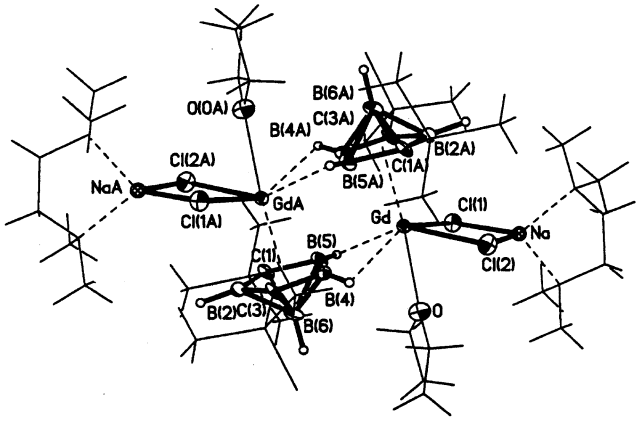

Fig. 35. Structure of $[\{\eta^5\text{-}2,4\text{-}(Me_3Si)_2C_2B_4H_4\}Gd(THF)(\mu\text{-}Cl)_2Na(TMEDA)]_2$ [45].

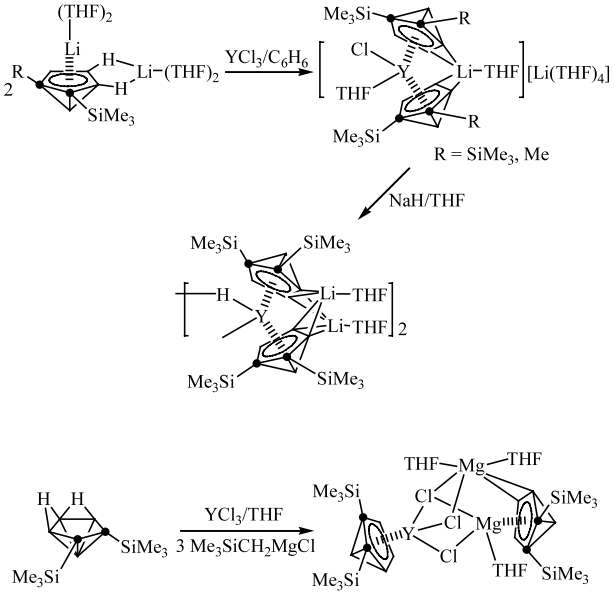

Scheme 21.

are not unusual compared with the corresponding lanthanacarboranes [46].

3. Metallacarboranes of actinides

3.1. C_2B_9 system

In comparison with metallacarboranes of d-block elements and lanthanides, the chemistry of metallacarboranes of actinides (also called actinacarboranes) is less studied although the first actinacarborane was reported in 1977 [47]. Reaction of UCl_4 with 2 equiv. of $Li_2[C_2B_9H_{11}]$ in THF gives $[Li(THF)_4]_2[(\eta^5\text{-}C_2B_9H_{11})_2UCl_2]$ which has been subjected to X-ray analysis (Scheme 22). As shown in Fig. 39, the U^{4+} ion is η^5-bonded to each of two carboranyl ligands and σ-bonded to two terminal chloro groups in a distorted-tetrahedral geometry with a ring centroid–U–ring centroid angle of 137°. The average U–cage atom and U–Cl distances are 2.73(2) and 2.599(6) Å, respectively. This also represented the first metallacarborane of f-block elements. There are no other reports in this field until 1996.

Reaction of $UBr_4(NCMe)_4$ with 2 equiv. of $Li_2[C_2B_9H_{11}]$ in THF affords a full-sandwich uranacarborane $[Li(THF)_4]_2[(\eta^5\text{-}C_2B_9H_{11})_2UBr_2]$ [48] (Scheme 22). An X-ray analysis reveals that its molecular structure is very similar to that of the corresponding chloro analogue (Fig. 40). The U^{4+} ion is η^5-bonded to each of two carboranyl ligands and σ-bonded to two terminal bromo groups in a highly distorted-tetrahedral

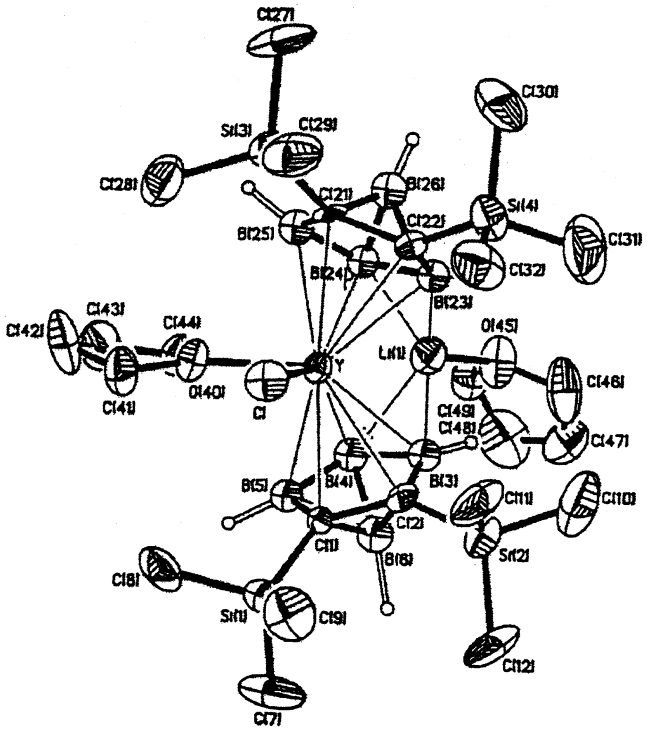

Fig. 36. Structure of $[\{[\eta^5\text{-}2,3\text{-}(Me_3Si)_2C_2B_4H_4]_2YCl(THF)\}\{Li(THF)\}]^-$ [46a].

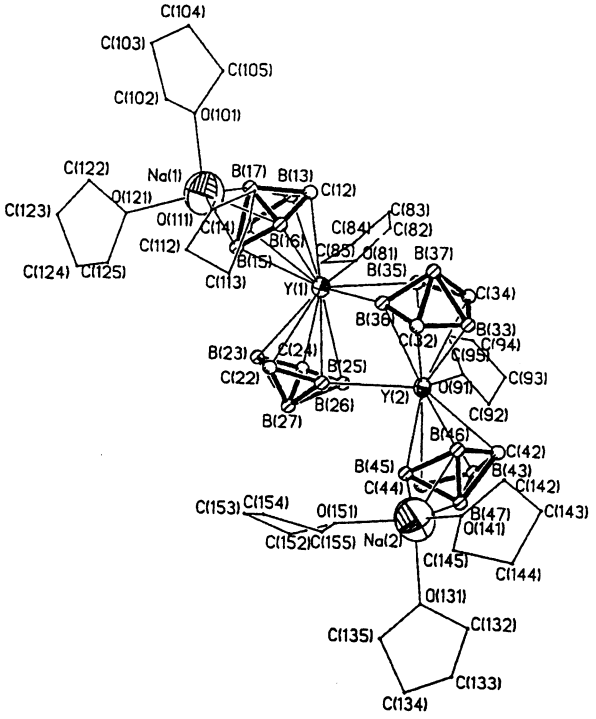

Fig. 37. Structure of $[\{[\eta^5\text{-}2,4\text{-}(Me_3Si)_2C_2B_4H_4]_2Y(THF)\}\{Na(THF)_3\}]_2$ [46a].

geometry with a ring centroid–U–ring centroid angle of 143.1°. The average U–cage atom and U–Br distances are 2.72(2) and 2.835(1) Å, respectively.

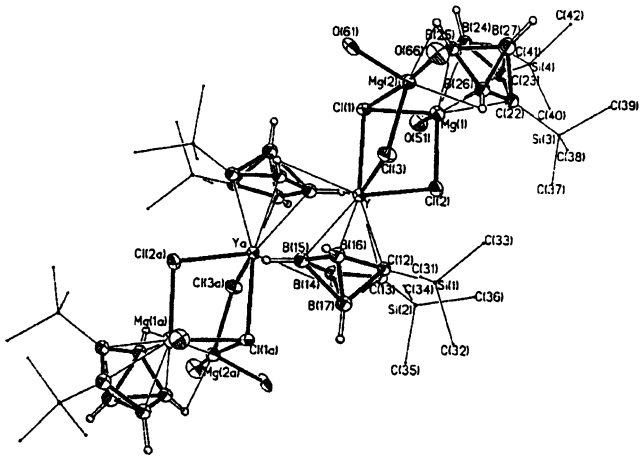

Fig. 38. Structure of $\{[\eta^5\text{-}2,3\text{-}(Me_3Si)_2C_2B_4H_4]Y(\mu\text{-}Cl)_3\}\{[\eta^5\text{-}2,3\text{-}(Me_3Si)_2C_2B_4H_4]Mg(THF)\}\{Mg(THF)_2\}$ [46a].

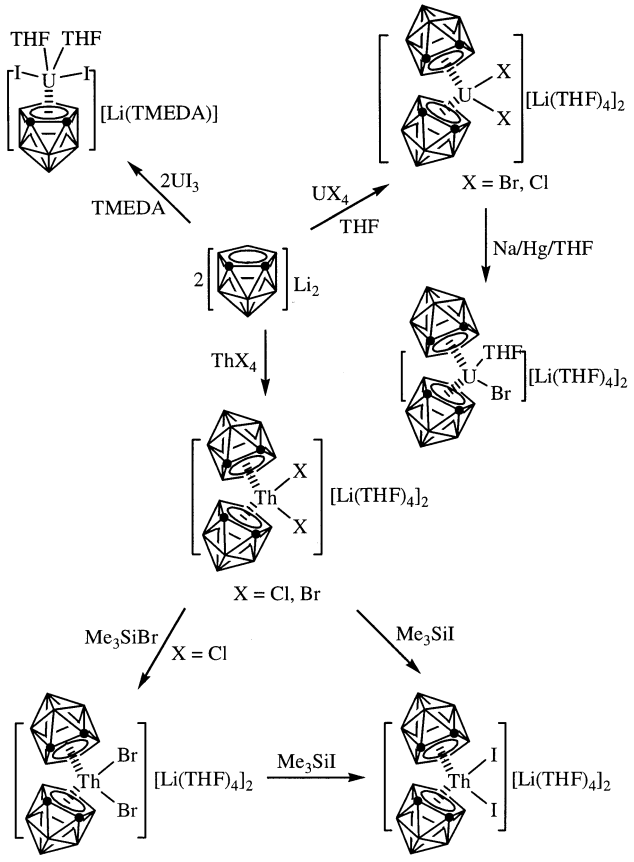

Scheme 22.

Reduction of $[Li(THF)_4]_2[(\eta^5\text{-}C_2B_9H_{11})_2UBr_2]$ by Na/Hg in THF produces a U(III) complex $[Li(THF)_4]_2[(\eta^5\text{-}C_2B_9H_{11})_2UBr(THF)]$ [49] (Scheme 22) which has been subjected to a single-crystal X-ray analysis. The U^{3+} ion is η^5-bonded to each of two carboranyl ligands and σ-bonded to one terminal bromo group and coordinated to one THF molecule in a distorted-tetrahedral geome-

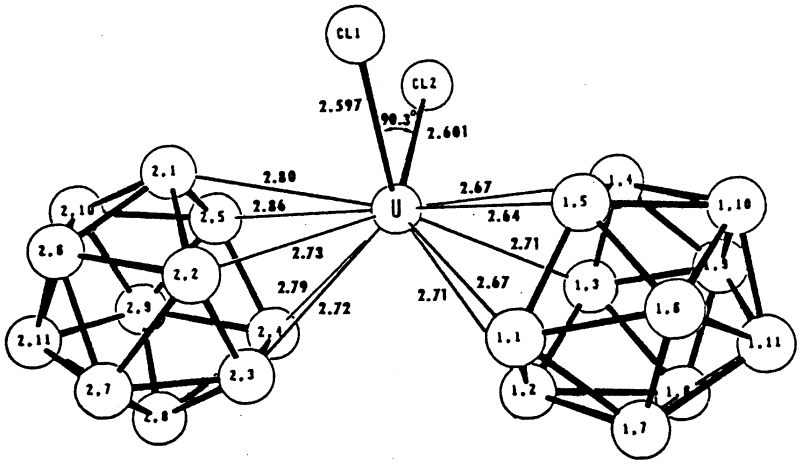

Fig. 39. Structure of $[(\eta^5\text{-}C_2B_9H_{11})_2UCl_2]^{2-}$ [47].

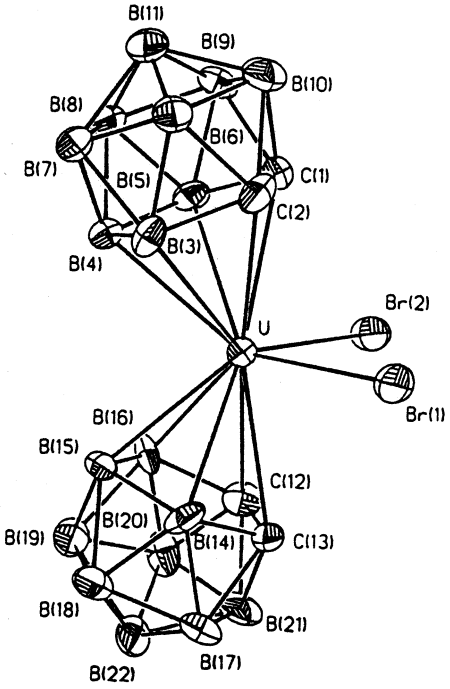

Fig. 40. Structure of $[(\eta^5\text{-}C_2B_9H_{11})_2UBr_2]^{2-}$ [48].

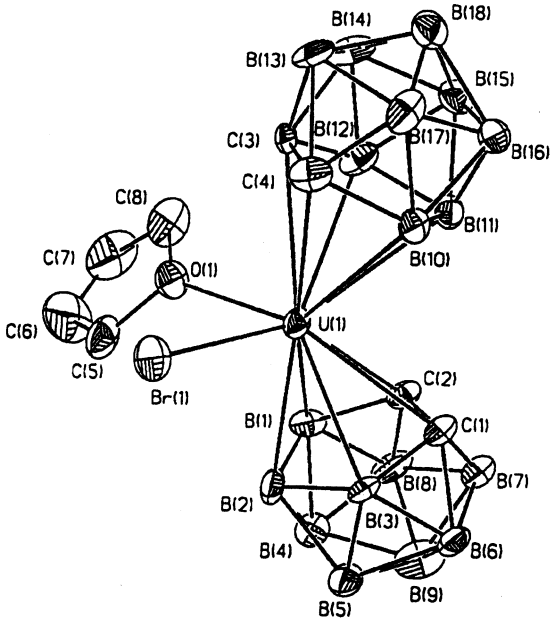

Fig. 41. Structure of $[(\eta^5\text{-}C_2B_9H_{11})_2UBr(THF)]^{2-}$ [49].

try with a ring centroid–U–ring centroid angle of 131.7° which is significantly smaller than the corresponding value of 143.1° in its parent complex (Fig. 41). The average U–cage atom and U–Br distances are 2.79(2) and 2.883(2) Å, respectively.

An equimolar reaction between $UI_3(THF)_4$ and $Li_2[Me_2C_2B_9H_9]$ in THF/TMEDA gives, after cation exchange with $(Ph_3P)_2NCl$, a half-sandwich uranacarborane $[(Ph_3P)_2N][(\eta^5\text{-}Me_2C_2B_9H_9)UI_2(THF)_2]$ [48] (Scheme 22). An X-ray diffraction study shows that the U^{3+} ion is η^5-bonded to one carboranyl ligand, σ-bonded to two terminal iodo units, and coordinated to two THF molecules in a highly distorted-square-pyramidal geometry (Fig. 42). The average U–cage atom and U–I distances are 2.79(2) and 3.143(1) Å, respectively.

Treatment of $ThBr_4(THF)_4$ with 2 equiv. of $Li_2[C_2B_9H_{11}]$ in THF yields a full-sandwich thoracarborane $[Li(THF)_4]_2[(\eta^5\text{-}C_2B_9H_{11})_2ThBr_2]$ [50] (Scheme 22), which can also be prepared by reacting the dichloro analogue with Me_3SiBr. Likewise, the diiodo derivative $[Li(THF)_4]_2[(\eta^5\text{-}C_2B_9H_{11})_2ThI_2]$ is readily obtained by treating either the dichloro or the dibromo complex with a slight excess of Me_3SiI. The driving forces for these substitution reactions are the large difference in bond dissociation energies between the reagents Me_3SiX (X = Br, I) and the byproduct Me_3SiCl. Fig. 43 shows that $(\eta^5\text{-}C_2B_9H_{11})_2ThBr_2^{2-}$ is isostructural with its uranium

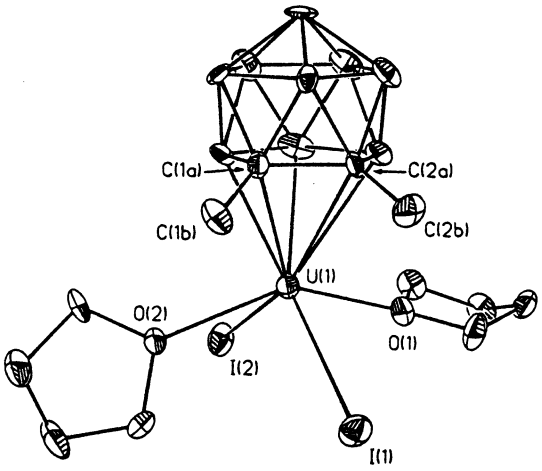

Fig. 42. Structure of $[(\eta^5\text{-}Me_2C_2B_9H_9)UI_2(THF)_2]^-$ [48].

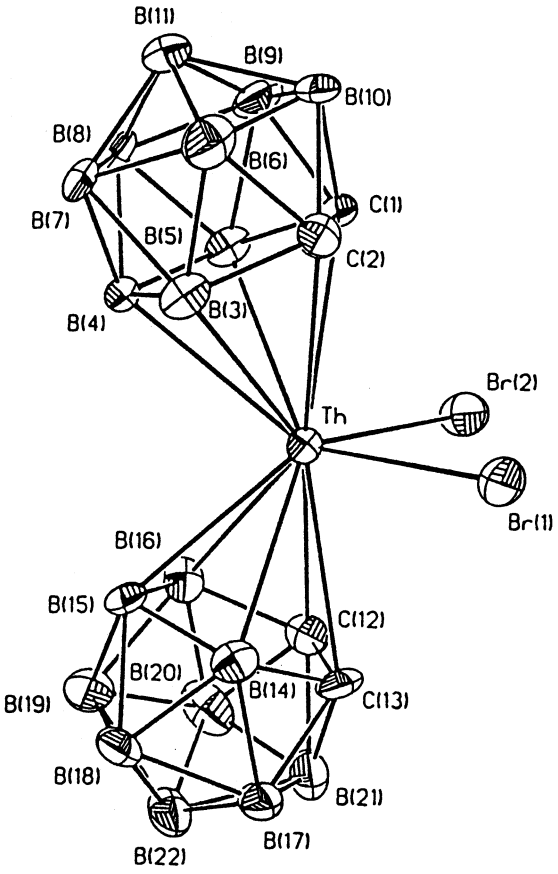

Fig. 43. Structure of $[(\eta^5\text{-}C_2B_9H_{11})_2ThBr_2]^{2-}$ [50].

analogue $(\eta^5\text{-}C_2B_9H_{11})_2UBr_2^{2-}$ and displays a bent-metallocene structure with a large ring centroid–Th–ring centroid angle of 142.4°. The average Th–cage atom and Th–Br distances are 2.774(14) and 2.869(1) Å, respectively.

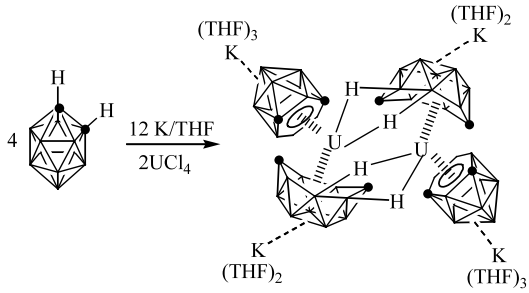

Scheme 23.

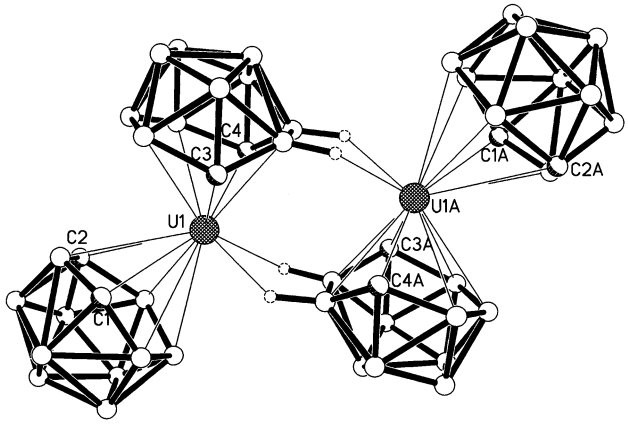

Fig. 44. Structure of $[(\eta^7\text{-}C_2B_{10}H_{12})(\eta^6\text{-}C_2B_{10}H_{12})U]_2^{4-}$ [51].

3.2. C_2B_{10} systems

The only known actinacarborane with C_2B_{10} systems is $[\{(\eta^7\text{-}C_2B_{10}H_{12})(\eta^6\text{-}C_2B_{10}H_{12})U\}\{K_2(THF)_5\}]_2$ which is prepared from the reaction of *o*-$C_2B_{10}H_{12}$ with excess K metal in THF, followed by treatment with a THF suspension of UCl_4 [51] (Scheme 23). An X-ray diffraction study reveals that it is a centrosymmetric dimer with a bent sandwich structural motif. As shown in Fig. 44, each U^{4+} ion is η^6-bonded to *nido*-$C_2B_{10}H_{12}^{2-}$, η^7-bonded to *arachno*-$C_2B_{10}H_{12}^{4-}$, and coordinated to two B–H bonds from the C_2B_5 bonding face of the neighboring *arachno*-$C_2B_{10}H_{12}^{4-}$ ligand in a highly distorted-tetrahedral geometry with a ring centroid–U–ring centroid angle of 136.3°. This complex represents not only the first metallacarborane containing a novel η^7-$C_2B_{10}H_{12}^{4-}$ ligand but also the first actinacarborane bearing a η^6-$C_2B_{10}H_{12}^{2-}$ ligand. It is not understood why the other *nido*-$C_2B_{10}H_{12}^{2-}$ dianion cannot be reduced to *arachno*-$C_2B_{10}H_{12}^{4-}$ tetraanion in the presence of excess K metal. It is assumed that this complex might represent an intermediate going from $(\eta^6\text{-}C_2B_{10}H_{12})_2U$ to $(\eta^7\text{-}C_2B_{10}H_{12})_2U^{4-}$.

The average U–cage atom (C_2B_4 bonding face) distance of 2.867(7) Å is longer than the average U–cage B atom (C_2B_5 bonding face) distance of 2.780(6) Å. The average U···B distance is 2.985(6) Å. The average U–C (C_2B_5 bonding face) distance is 2.429(5) Å, which

is at the short end of typical U–C σ bond distances normally observed in organouranium complexes.

4. Conclusions and perspectives

The chemistry of metallacarboranes of f-block elements has made considerable progress in the past 10 years or so. Many lanthanacarboranes and actinacarboranes with novel structural features have been prepared. Owing to the large size of f-block elements and unique properties of carborane cage molecules, steric factors often dominate the bonding interactions between the metal ions and carboranyl ligands.

Carboranyl ligands are capable of being bonded to metal ions in η^7-, η^6-, η^5-, and σ-fashion, which makes the chemistry of metallacarboranes of f-block elements richer and more complex in comparison with traditional organo-f-element chemistry. On the other hand, subtle changes in the reaction conditions can lead to the production of very different products, particularly if the C_2B_4 ligand systems are involved.

Although numerous metallacarboranes of f-block elements have been prepared and structurally characterized, there are still some synthetic challenges that remain within this area of chemistry: no definite lanthanacarboranes or actinacarboranes containing M–C or M–H σ bonds are reported, and the carboranyl ligands are limited to C_2B_4-, C_2B_9- and C_2B_{10}-systems only.

Synthetic, structural and bonding curiosities are the main research activities in this field in the past decade and may also be the research focus in the future. The chemical properties of metallacarboranes of f-block elements are largely unexplored and would certainly attract chemists' attention after the synthetic routes to the M–C σ bond containing lanthanacarboranes and actinacarboranes have been realized. The search for applications of these metallacarboranes in many disciplines such as electronics, ceramics, catalysis, polymers and high energy fuel additives, etc., is anticipated in the future.

Acknowledgements

I would like to thank my motivated and talented students who have performed most of the research described in this article and whose names are cited in the references. I also thank the Research Grants Council of the Hong Kong Special Administration Region, Direct Grant and Chemistry Department of the Chinese University of Hong Kong for financial support. I am grateful to my collaborators with whom I have had the pleasure to interact.

References

[1] M.F. Hawthorne, D.C. Young, P.A. Wegner, J. Am. Chem. Soc. 87 (1965) 1818.
[2] (a) R.N. Grimes, in: E.W. Abel, F.G.A. Stone, G. Wilkinson (Eds.), Comprehensive Organometallic Chemistry II, vol. 1 (chapter 9), Pergamon Press, Oxford, UK, 1995;
(b) R.N. Grimes, Coord. Chem. Rev. 200/202 (2000) 773.
[3] (a) A.K. Saxena, N.S. Hosmane, Chem. Rev. 93 (1993) 1081;
(b) A.K. Saxena, J.A. Maguire, N.S. Hosmane, Chem. Rev. 97 (1997) 2421;
(c) N.S. Hosmane, J.A. Maguire, J. Cluster Sci. 4 (1993) 297.
[4] (a) H. Schumann, J.A. Meese-Marktscheffel, L. Esser, Chem. Rev. 95 (1995) 865;
(b) F.T. Edelmann, in: E.W. Abel, F.G.A. Stone, G. Wilkinson (Eds.), Comprehensive Organometallic Chemistry II, vol. 4, Pergamon Press, Oxford, UK, 1995, p. 11.
[5] M.F. Hawthorne, D.C. Young, T.D. Andrews, D.V. Howe, R.L. Pilling, A.D. Pitts, M. Reintjes, L.F. Warren, Jr., P.A. Wegner, J. Am. Chem. Soc. 90 (1968) 879.
[6] M.J. Manning, C.B. Knobler, M.F. Hawthorne, J. Am. Chem. Soc. 110 (1988) 4458.
[7] M.J. Manning, C.B. Knobler, R. Khattar, M.F. Hawthorne, Inorg. Chem. 30 (1991) 2009.
[8] W.J. Evans, Coord. Chem. Rev. 206 (2000) 263.
[9] Z. Xie, Z. Liu, K.-y. Chiu, F. Xue, T.C.W. Mak, Organometallics 16 (1997) 2460.
[10] K.-y. Chiu, M. Phil. Thesis, The Chinese University of Hong Kong, Hong Kong, China, 1997.
[11] (a) J. Scholz, A. Scholz, R. Weimann, C. Janiak, H. Schumann, Angew. Chem. Int. Ed. Engl. 33 (1994) 1171;
(b) H.J. Heeres, A. Meetsma, J.H. Teuben, Angew. Chem. Int. Ed. Engl. 29 (1990) 420;
(c) M.R. Gagne, C.L. Stern, T.J. Marks, J. Am. Chem. Soc. 114 (1992) 275.
[12] K.-y. Chiu, Z. Zhang, T.C.W. Mak, Z. Xie, J. Organomet. Chem. 614/615 (2000) 107.
[13] G.C. Bazan, W.P. Schaefer, J.E. Bercaw, Organometallics 12 (1993) 2126.
[14] Z. Xie, Z. Liu, Q. Yang, T.C.W. Mak, Organometallics 18 (1999) 3603.
[15] K.F. Shaw, B.D. Reid, A.J. Welch, J. Organomet. Chem. 482 (1994) 207.
[16] V.N. Lebedev, N.F. Shemyakin, S.P. Soldovnikov, L.I. Zakharkin, Metalloorg. Khim. 1 (1988) 718.
[17] R. Khattar, C.B. Knobler, S.E. Johnson, M.F. Hawthorne, Inorg. Chem. 30 (1991) 1970.
[18] R. Khattar, M.J. Manning, C.B. Knobler, S.E. Johnson, M.F. Hawthorne, Inorg. Chem. 31 (1992) 268.
[19] K. Chui, H.W. Li, Z. Xie, Organometallics 19 (2000) 5447.
[20] Z. Xie, S. Wang, Z. Zhou, F. Xue, T.C.W. Mak, Organometallics 17 (1998) 489.
[21] Z. Xie, S. Wang, Z. Zhou, T.C.W. Mak, Organometallics 18 (1999) 1641.
[22] Z. Xie, S. Wang, Z. Zhou, T.C.W. Mak, Organometallics 17 (1998) 1907.
[23] Z. Xie, S. Wang, Q. Yang, T.C.W. Mak, Organometallics 18 (1999) 2420.
[24] Z. Xie, S. Wang, Q. Yang, T.C.W. Mak, Organometallics 18 (1999) 1578.
[25] S. Wang, Q. Yang, T.C.W. Mak, Z. Xie, Organometallics 18 (1999) 4478.
[26] K. Chui, Q. Yang, T.C.W. Mak, Z. Xie, Organometallics 19 (2000) 1391.
[27] E. Hong, Y. Kim, Y. Do, Organometallics 17 (1998) 2933.

[28] Z. Xie, K. Chui, Q. Yang, T.C.W. Mak, Organometallics 18 (1999) 3947.
[29] S. Wang, Z. Xie, unpublished results.
[30] S. Wang, H.W. Li, Z. Xie, Organometallics 20 (2001) 3624.
[31] G. Zi, H.W. Li, Z. Xie, Organometallics 20 (2001) 3836.
[32] G. Zi, H.W. Li, Z. Xie, Chem. Commun. (2001) 1110.
[33] G. Zi, Z. Xie, unpublished results.
[34] (a) K. Wade, Adv. Inorg. Chem. Radiochem. 18 (1976) 1;
(b) R.E. Williams, Adv. Inorg. Chem. Radiochem. 18 (1976) 67.
[35] W.J. Evans, M.F. Hawthorne, J. Chem. Soc. Chem. Commun. (1974) 38.
[36] K. Chui, Q. Yang, T.C.W. Mak, W.H. Lam, Z. Lin, Z. Xie, J. Am. Chem. Soc. 122 (2000) 5758.
[37] S. Wang, H.W. Li, Z. Xie, Organometallics 20 (2001) 3842.
[38] A.R. Oki, H. Zhang, N.S. Hosmane, Angew. Chem. Int. Ed. Engl. 31 (1992) 432.
[39] (a) H. Zhang, A.R. Oki, Y. Wang, J.A. Maguire, N.S. Hosmane, Acta Crystallogr. Sect. C 51 (1995) 635.
(b) C. Zheng, N.S. Hosmane, H. Zhang, D. Zhu, J.A. Maguire, Internet J. Chem. 2 (1999).
[40] N.S. Hosmane, Y. Wang, A.R. Oki, H. Zhang, J.A. Maguire, Organometallics 15 (1996) 626.
[41] N.S. Hosmane, A.R. Oki, H. Zhang, Inorg. Chem. Commun. 1 (1998) 101.
[42] (a) N.S. Hosmane, Y. Wang, H. Zhang, J.A. Maguire, M. McInnis, T.G. Gray, J.D. Collins, Organometallics 15 (1996) 1006;
(b) N.S. Hosmane, Y. Wang, H. Zhang, Y. Zhu, J.A. Maguire, Inorg. Chem. Commun. 4 (2001) 547.
[43] N.S. Hosmane, Y. Wang, H. Zhang, A.R. Oki, J.A. Maguire, E. Waldhör, W. Kain, H. Binder, R.K. Kremer, Organometallics 14 (1995) 1101.
[44] H. Zhang, Y. Wang, J.A. Maguire, N.S. Hosmane, Acta Crystallogr. Sect. C 52 (1996) 8.
[45] N.S. Hosmane, S. Li, C. Zheng, J.A. Maguire, Inorg. Chem. Commun. 4 (2001) 104.
[46] (a) N.S. Hosmane, D. Zhu, H. Zhang, A.R. Oki, J.A. Maguire, Organometallics 17 (1998) 3196;
(b) A.R. Oki, H. Zhang, N.S. Hosmane, Organometallics 10 (1991) 3964.
[47] F.R. Fronczek, G.W. Halstead, K.N. Raymond, J. Am. Chem. Soc. 99 (1977) 1769.
[48] D. Rabinovich, C.M. Haswell, B.L. Scott, R.L. Miller, J.B. Nielsen, K.D. Abney, Inorg. Chem. 35 (1996) 1425.
[49] F.M. de Rege, W.H. Smith, B.L. Scott, J.B. Nielsen, K.D. Abney, Inorg. Chem. 37 (1998) 3664.
[50] D. Rabinovich, R.M. Chamberlin, B.L. Scott, J.B. Nielsen, K.D. Abney, Inorg. Chem. 36 (1997) 4216.
[51] Z. Xie, C. Yan, Q. Yang, T.C.W. Mak, Angew. Chem. Int. Ed. 38 (1999) 1761.